GEMAS: Geochemical background and mineral potential of emerging tech-critical elements in Europe revealed from low-sampling density geochemical mapping

Philippe Négrel, Anna Ladenberger, Clemens Reimann, Manfred Birke, Alecos Demetriades, Martiya Sadeghi

▶ **To cite this version:**

HAL Id: hal-02735002
https://brgm.hal.science/hal-02735002

Submitted on 20 Jul 2022

1 # GEMAS: Geochemical background and mineral potential of

2 # emerging tech-critical elements in Europe revealed from low-

3 # sampling density geochemical mapping

4

5 **Philippe NÉGREL[1,‡], Anna LADENBERGER[2], Clemens REIMANN[3], Manfred BIRKE[4],**

6 **Alecos DEMETRIADES[5], Martiya SADEGHI[2] and The GEMAS Project Team[6]**

7

8 [1]BRGM, Laboratories Division, Orléans, France, p.negrel@brgm.fr

9 [2]Geological Survey of Sweden, Uppsala, Sweden, anna.ladenberger@sgu.se,

10 martiya.sadeghi@sgu.se

11 [3]Geological Survey of Norway, Trondheim, Norway, clemensreimann@yahoo.co.uk (retired)

12 [4]Bundesanstalt für Geowissenschaften und Rohstoffe, Stillweg 2, 30655 Hannover,

13 Germany, Manfred.Birke@bgr.de

14 [5]Institute of Geology and Mineral Exploration, 1 Spirou Louis St., Olympic Village, Acharnae,

15 13677 Athens, Hellas, alecos.demetriades@gmail.com (retired)

16

17 [6] *The GEMAS Project Team*: S. Albanese, M. Andersson, R. Baritz, M.J. Batista, B. Flem, A.

18 Bel-lan, D. Cicchella, B. De Vivo, W. De Vos, E. Dinelli, M. Ďuriš, A. Dusza-Dobek, O.A.

19 Eggen, M. Eklund, V. Ernstsen, P. Filzmoser, D.M.A. Flight, S. Forrester, M. Fuchs, U. Fügedi,

20 A. Gilucis, M. Gosar, V. Gregorauskiene, W. De Groot, A. Gulan, J. Halamić, E. Haslinger, P.

21 Hayoz, R. Hoffmann, J. Hoogewerff, H. Hrvatovic, S. Husnjak, L. Janik, G. Jordan, M.

22 Kaminari, J. Kirby, J. Kivisilla, V. Klos, F. Krone, P. Kwećko, L. Kuti, A. Lima, J. Locutura,

23 D. P. Lucivjansky, A. Mann, D. Mackovych, J., Matschullat, M. McLaughlin, B.I. Malyuk, R.

24 Maquil, R.G. Meuli, G. Mol, P. O'Connor, R. K. Oorts, R.T. Ottesen, A. Pasieczna, W.

25 Petersell, S. Pfleiderer, M. Poňavič, S. Pramuka, C. Prazeres, U. Rauch, S. Radusinović, I.

26 Salpeteur, R. Scanlon, A. Schedl, A.J. Scheib, I. Schoeters, P. Šefčik, E Sellersjö, F. Skopljak,

27 I. Slaninka, A. Šorša, R. Srvkota, T. Stafilov, T. Tarvainen, V. Trendavilov, P. Valera, V.

28 Verougstraete, D. Vidojević, A. Zissimos and Z. Zomeni.

29

30

31

‡ corresponding author

Abstract

The demand for 'high-tech' element resources (e.g., rare earth elements, lithium, platinum group elements) has increased with their continued consumption in developed countries and the emergence of developing economies. To provide a sound knowledge base for future generations, it is necessary to identify the spatial distribution of critical elements at a broad-scale, and to delineate areas for follow-up surveys. Subsequently, this knowledge can be used to study possible environmental consequences of the increased use of these resources.

In this paper, three critical industrial elements (Sb, W, Li) from low-sampling density geochemical mapping at the continental-scale are presented. The geochemical distribution and spatial patterns have been obtained from agricultural soil samples (Ap-horizon, 0–20 cm; N=2108 samples) collected at a density of 1 site per 2500 km^2 and analysed by ICP-MS after a hot aqua regia digestion as part of the GEMAS (GEochemical Mapping of Agricultural and grazing land Soil) soil-mapping project in 33 European countries. Most of the geochemical maps show exclusively natural background element concentrations with minor, or without, anthropogenic influence. The maximum extent of the last glaciation is marked as a discrete element concentration break, and a distinct difference occurs in element concentration levels between the soil of northern and southern Europe, most likely an effect of soil genesis, age and weathering. The Sb, W and Li concentrations in soil provide a general overview of element spatial distribution in relation to complexity of the underlying bedrock and element mobility in the surface environment at the continental-scale. The chemical composition of agricultural soil represents largely the primary mineralogy of the source bedrock, the effects of pre- and post-depositional chemical weathering, formation of secondary products, such as clays, and element mobility, either by leaching or mineral sorting. Observed geochemical patterns of Li, W and Sb can be often linked with known mineralisation as recorded in the ProMine Mineral Database, where elements in question occur either as main or secondary resources. Anthropogenic impact has only been identified locally, predominantly in the vicinity of large urban agglomerations. Unexplained high element concentrations may potentially indicate new sources for high-tech elements and should be investigated at a more detailed scale.

Keywords: agricultural soil, weathering, geochemistry, critical elements, antimony, tungsten, lithium

1. Introduction

The demands for a variety of mineral and/or element resources (rare earth elements, platinum group elements, cobalt, beryllium, lithium, iodine, etc.) are strongly increasing (Buchert et al., 2009; Bertrand et al., 2016; Meinert et al., 2016). These elements are essential for maintaining and improving the present and future quality of life, including many high-technology yet low-carbon industries. Two factors have been used by the National Research Council (NRC) to rank criticality: (a) the degree to which a commodity is essential and (b) the risk of supply disruption for the commodity (Ali et al., 2017). Further, the demand for energy-related minerals has increased, as global energy production diversifies beyond carbon and nuclear-based sources (Teske, 2019). Many of these elements are crucial to a variety of manufacturing, high-tech and military applications like photovoltaic solar cells (Ga, Ge, In, Se, Ag, Te), high-strength permanent magnets and magnetic and/or optical components for lighting (mostly rare earth elements and Co), for wind turbines and hybrid automobiles, high performance batteries (Li, La), catalysts (Pt, Pd, Ce), advanced turbines (Re), and advanced energy reactor designs (He). A critical mineral and/or element is both essential in use, subject to the risk of supply restriction and the induction of environmental impacts. Based on information about occurrences, resources and reserves, extraction, processing, utilisation, and recycling, good candidates for the designation of 'energy-critical' elements can be determined. The list of critical raw materials (Table 1) is updated by the European Union Commission every few years with the last update in 2017 (European Commission, 2017).

The overall results of the 2017 criticality assessment are shown in Fig. 1 where the critical raw materials are denoted by the red dots (European Commission, 2017). Of the 61 candidate raw materials assessed (58 individual and 3 grouped materials, biotic and abiotic), the following 26 raw materials and groups of raw materials were identified as critical (Table 1). It is noted that Li discussed here is not yet a critical raw material, according to the 2017

3

92 European Commission classification, but its criticality is being discussed in view of its

93 importance as a critical element for future sustainable technologies according to UNEP (2009).

94 Lithium is an essential, in fact a critical, element in the battery industry and in technical

95 evolution towards low-carbon society.

96
97 *Table 1. List of Critical Raw Materials, updated in 2017 by the European Commission*
98 *(2017).*
99

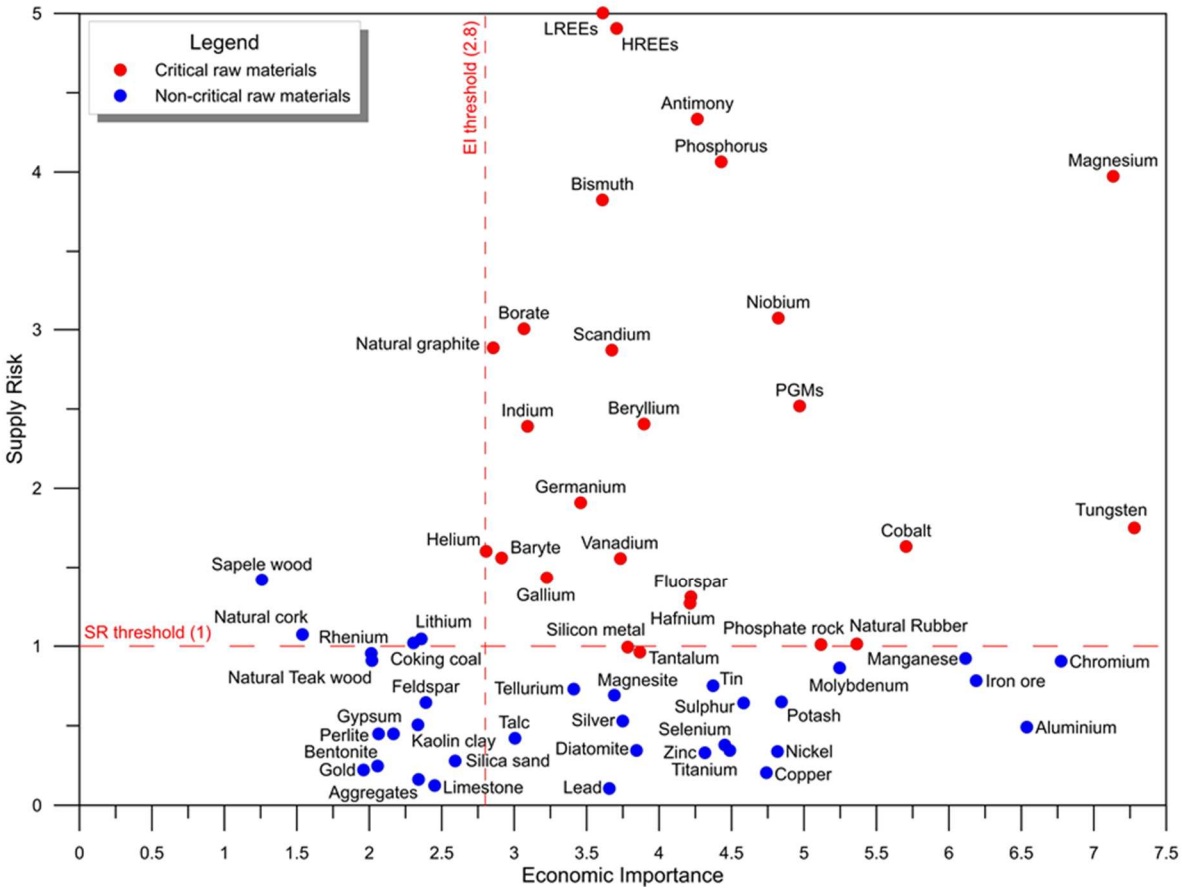| 2017 Critical Raw Materials				
Antimony	Cobalt	Helium	Natural graphite	Phosphorus
Baryte	Fluorspar	HREEs	Natural Rubber	Scandium
Beryllium	Gallium	Indium	Niobium	Silicon metal
Bismuth	Germanium	LREEs	PGMs	Tantalum
Borate	Hafnium	Magnesium	Phosphate rock	Tungsten
				Vanadium

100

101
102
103 *Figure 1. Criticality assessment of economically important raw materials for the European*
104 *Union in 2017 (redrawn from European Commission, 2017, Fig. 6, p.39).*
105

106   Geoscientists have a prominent role in the exploration for, management of, and

107   environmentally safe handling of critical mineral and/or element resources considering that

108   these needs will become even more important as the world's population and standards of living

109   continue to increase (Nickless et al., 2015; Ali et al., 2017). It is worth noting that the concept

110   of criticality is variable (and to large degree political) and depends principally on the context.

111   What is critical for a state, a manufacturer or a product may not be critical for another, and what

112   is critical for national defence may be different when compared to what is necessary to make

113   an electronic apparatus cheaper. Therefore, prioritisation of critical minerals and/or elements

114   are crucial for modern societies and has important implications for our economic prosperity

115   (Bringezu et al., 2016).

116   To provide a solid resource base for the future, but also to timely identify any possible

117   new environmental impact of the increased use of these elements, it is necessary to identify

118   their natural spatial distribution with a wider view, from the order of a country or a continental

119   block, e.g., European Union (Lambert et al., 2013). Any significant change in their cycle at the

120   Earth's surface, due to their increased use in a variety of technological applications, needs

121   robust preliminary knowledge. The growing consumption of critical elements generates the

122   demand for new production, both from primary (ore deposits) and secondary (mineral-based

123   and non-mineral-based wastes) sources. At some point, they may become new contaminants

124   and their identification in various environmental compartments is an urgent issue for future

125   pollution and waste management.

126   The chemical elements, which are now key components for the development of new

127   technologies, are according to the present understanding of their concentrations, transformation

128   and transport in the different environmental compartments, poorly studied (Reimann et al.,

129   2010). This paper presents the GEMAS (Geochemical Mapping of Agricultural and grazing

130   land Soil) results for Li, W and Sb, a project carried out by the Geochemistry Expert Group of

131   EuroGeoSurveys in cooperation with Eurometaux (European Association of Metals). The

132   GEMAS project aims were to detect and to map the element variation in productive soil at the

133   European scale. Soil samples were collected from 33 European countries, covering an area of

134   5.6 million km^2 (Reimann et al., 2012a; 2014a, b). Reimann et al. (2016) argue for low sampling

135   densities (1 site/100 to 1 site/18 000 km^2) rather than the costly and time-consuming very high

136   sampling densities (100s to 1000s of samples/km^2) employed for geochemical exploration,

137   giving the same conclusions as those obtained in previous studies of geochemical mapping in

138   continental- and regional-scale surveys (Smith and Reimann, 2008; Garrett et al., 2008;

139   Cicchella et al., 2013; Birke et al., 2015). Reimann et al. (2007a, 2016) stated that this low-

140   sampling density geochemical survey approach has also proved efficient in the early stages of

141   mineral exploration programmes through identification of more suitable regions for detailed

142   mineral exploration.

143   As part of GEMAS valorisation, a series of peer-reviewed publications, where detailed

144   interpretation of the continental-scale distribution of single elements or related groups of

145   elements, have been published, e.g., Reimann et al. (2012b - Pb); Ottesen et al. (2013 - Hg);

146   Tarvainen et al. (2013 - As); Scheib (2012 - Nb); Sadeghi et al. (2013 - Ce, La, Y); Birke et al.

147   (2014a, 2016, 2017 – Cd); Poňavič and Scheib (2014 – Se); Cichella et al. (2014 – U, Th, K);

148   Ladenberger et al. (2015 - In); Albanese et al. (2015 - Cr, Ni, Co, Cu); Négrel et al. (2016 – Ge;

149   2018a – U, Th; 2018b - Rb, Ga, Cs); Jordan et al. (2018 – Ni). Among these publications, the

150   elements In, Nb, Ge and the rare earth elements, although defined as technology-critical

151   elements, have been interpreted in the frame of weathering patterns related to climate and

152   inheritance from processes controlling element binding to mineral phases.

153   Even if we are not facing an imminent absolute shortage of energy critical elements

154   (e.g., see the Hubbert's Peak scenario in Hubbert, 1982), market-driven shortages are possible,

155   and no country can become independent from energy critical elements, which are nowadays

156 produced often in politically unstable countries. Therefore, securing energy critical elements

157 requires an advanced research plan including geological, metallurgical and materials science,

158 the impact of which on knowledge and, therefore, the capacity to exploit resources is crucial

159 for future development (Nickless et al., 2015; Ali et al., 2017). In this paper, we investigate the

160 geochemical distribution and behaviour of three critical elements Sb, W and Li using low-

161 sampling density geochemical mapping at the continental-scale and interpret the geochemical

162 patterns in relation to their mineral potential. We need to point out the difference between a

163 single mineralisation event, which cannot be located by using the GEMAS density of 1

164 sample/2500 km^2 and a mineralising process which affects a much larger area, a mineral

165 province that can be identified with this data set (Bölviken et al., 1990). The GEMAS data set

166 make it possible to define, therefore, potential areas, where follow-up and detailed

167 geochemical exploration survey can be carried out in order to better define the mineralised

168 zones (Reimann et al., 2007b).

2. Materials and methods

170 The GEMAS project (Reimann et al., 2014a, b) was carried out by the Geochemistry Expert

171 Group of EuroGeoSurveys in cooperation with Eurometaux (European Association of Metals)

172 and managed by the Geological Survey of Norway (NGU). It was the second large geochemical

173 mapping survey at the European continental-scale following the FOREGS project (Salminen,

174 Tarvainen et al., 1998; Salminen et al., 2005; De Vos, Tarvainen et al., 2006). Agricultural and

175 grazing land soil samples were collected in 33 European countries, covering an area of about

176 5.6 million km^2 (Reimann et al., 2012a; 2014a, b). The survey area is shown in Figure 2. The

177 main objective of the project was to detect and to map the element variation in agricultural and

178 grazing land soil and to present their geochemical baseline variation for Europe. The soil

179 samples were not taken at known contaminated sites, in the immediate vicinity of industry or

180 power plants, cities, railway lines or major roads, directly below high power electric lines or

181 near to pylons and wooden fences. The GEMAS aqua regia and XRF results are provided in a

182 two-volume geochemical atlas (Reimann et al., 2014a, b).

183   For the GEMAS project two types of soil samples from two land use categories have

184 been collected at an average density of 1 site per 2500 km^2 each (Fig. 2b). Grazing land soil

185 (Gr; N=2024 samples) has been defined as 'land under permanent grass cover' and a sample

186 depth of 0–10 cm was used, according to the REACH regulation (Registration, Evaluation,

187 Authorisation and Restriction of chemicals) guidance document requirements

188 (https://echa.europa.eu/). Agricultural soil (Ap; N=2108 samples) was collected from the

189 ploughing layer of an agricultural arable field from a depth of 0–20 cm. Each sample (ca 3.5

190 kg) corresponds to a composite of five sub-samples taken from the corners and centre of a

191 10×10 m square. Field duplicate samples were collected from both land use categories at a rate

192 of 1 in 20 routine samples.

Figure 2. Modified from Négrel et al. (2015, Fig. 1, p.3). (a) Map of parent materials in Europe showing the distribution of various lithologies across the continent (modified from Gunther et al., 2013 and adapted from Négrel et al., 2015, Fig. 1, p.3). (b) Sample locations (dots) of the ploughed agricultural soil (Ap-samples; N=2108). Map projection: Lambert Azimuthal Equal Area (ETRS_1989_LAEA), with central meridian at 10°. (c) Generalised geological map of Europe with major lithotectonic units, Variscan and Alpine belts, Transeuropean Suture Zone (TESZ) and the extension of maximum glaciation (modified from Reimann et al., 2012b, Fig. 1, p.533).

A single facility (State Geological Institute of Dionyz Stur, Slovakia) prepared all samples for analysis. Soil samples were air-dried, sieved to <2 mm using a nylon screen, homogenised and finally split into 10 sub-samples. Two reference materials, e.g., standards, prepared in the same laboratory, were inserted at a rate of 1 in 20 samples together with field

208   and analytical replicates to monitor analytical performance during the project. Samples were

209   analysed by total X-ray fluorescence (XRF) and partial extraction methods like aqua regia (AR)

210   and mobile metal ion (MMI®) (Reimann et al., 2012a; 2014a, b), and here the results of the AR

211   method will be discussed.

212   The aqua regia extraction applied to the soil samples prior to analysis used a 15 g aliquot

213   of the unmilled <2 mm fraction, which was leached in 90 ml of aqua regia (95°C, 1 hour) and

214   then made up to a final volume of 300 ml with 5% HCl. The solutions were analysed using a

215   combination of inductively coupled plasma-atomic emission spectrometry (ICP-AES) and

216   inductively coupled plasma-mass spectrometry (ICP-MS) at ACME laboratories in Vancouver,

217   Canada (now Bureau Veritas Mineral Laboratories). A total of 53 elements was determined on

218   the over 5000 soil samples using matrix matched standards and reference materials.

219   A rigorous quality control (QC) procedure was part of the analytical protocol (Reimann

220   et al., 2009; Demetriades et al., 2014). Samples were analysed in batches consisting of 20

221   samples (Reimann et al., 2009). In each batch, one field duplicate, one analytical replicate of

222   the field duplicate and a project standard were inserted. The practical detection limit (PDL) was

223   estimated from results of the project replicate samples by calculating regression line coefficients

224   with the 'reduced major axis line' procedure (Demetriades, 2011). This PDL in the aqua regia

225   extraction by ICP-MS is 0.003 mg/kg for Sb, 0.01 mg/kg for W and 0.04 mg/kg for Li. Details

226   on analytical procedures and quality control are provided in Reimann et al. (2009; 2011; 2012c),

227   Birke et al. (2014b) and Demetriades et al. (2014).

228   Geochemical data are compositional data, element concentrations reported in wt % or

229   mg/kg sum up to a constant and are thus not free to vary (Reimann et al., 2012d). Compositional

230   data do not plot in the Euclidean space, but rather on the Aitchison simplex (Aitchison, 1986;

231   Buccianti et al., 2006; Pawlowsky-Glahn and Buccianti, 2011). Thus, only order statistics

232   should be used in statistical data processing. The colour surface maps were produced by kriging,

233 based on a careful variogram analysis (Filzmoser et al., 2014). Kriging was used to interpolate

234 values from the irregularly distributed sampling sites to a regular grid and into unsampled space.

235 Class boundaries for the colour surface maps are based on percentiles (5, 25, 50, 75, 90 and 95).

236 Geochemical maps displayed hereafter (Figs. 4-6) were produced in ArcGIS.

237 **3. Results and discussion**

238 **3.1. Element concentrations in agricultural soil**

239 The concentrations of Sb, W and Li generated by the GEMAS project constitute a homogeneous

240 data set and can be compared, but are not compatible, with other continental data sets, e.g., from

241 Europe (FOREGS; Salminen et al., 2005; De Vos, Tarvainen et al., 2006), U.S.A. (Smith et al.,

242 2013, 2014), Australia (Caritat and Cooper (2011a, b, c, d) and China (Xie et al., 2012) as

243 tabulated in Table 2.

244

245 3.1.1. Sb concentrations in agricultural soil

246 The median for Sb in the Ap and Gr soil samples in Europe in the hot aqua regia

247 extraction are very close, 0.234 and 0.275 mg/kg, respectively. The combined plot histogram -

248 density trace one - dimensional scattergram - boxplot shows the univariate Sb data distribution

249 (Fig. 3a for Ap, and 3b for Gr samples). The existence of outliers in the Sb distribution is shown

250 by one-dimensional scattergram and boxplot. The density trace displays a smooth multimodal

251 distribution, but is overall symmetrical about the median, a feature also indicated by the very

252 symmetrical boxplot (log-scale). Compared to the upper continental crust (UCC) estimated Sb

253 abundance of 0.4 mg/kg (Hu and Gao, 2008), the aqua regia extractable Sb (median Ap 0.234

254 and Gr 0.275 mg/kg) is lower by a factor of 1.74 in the Ap samples, and 1.45 in the Gr soil

255 samples. Due to high detection limits of GEMAS XRF results, it is not possible to directly relate

256 GEMAS total concentrations to the UCC values. However, estimated extractability of Sb (from

11

257 the comparison of aqua regia and XRF results) is 9 and 13% for the Ap and Gr samples,

258 respectively (Reimann et al., 2011).

259 Table 2. Median values of Sb, W and Li (in mg/kg) from continental-scale geochemical surveys.
260

Provenance	Analytical information	Sb median (Sb range)	W median (W range)	Li median (Li range)	Source
World soil	<2 mm, total, estimate	1 (<0.2 – 10)	1.5 (0.5 – 83)	25 (3 – 350)	Bowen (1979)
FOREGS[1]-Atlas, EU, topsoil (0 - 25 cm)	<2 mm, total (ICP-MS[2], N=845)	0.6 (<0.02 – 31.1)	<5.0[3] (<5.0 – 14)[3]	20.8 (0.28-271)[4]	Salminen et al. (2005)
GEMAS[5], EU, agricultural soil (0 – 20 cm)	<2 mm, AR[4] (ICP-MS[2], N = 2108)	0.23 (<0.02 – 17)	0.073 (<0.01 – 5.2)	11.4 (0.161 – 136)	Reimann et al. (2014a)
GEMAS, EU, agricultural soil (0 – 20 cm)	<2 mm, total XRF (N = 2108)	<5 (<0.5 – 36)	<5 (5 – 25)	n.d.	Reimann et al. (2014a)
GEMAS[5], EU, grazing land soil (0 – 10 cm)	<2 mm, AR[4] (ICP-MS[2], N = 2024)	0.28 (<0.02 – 25)	0.077 (<0.01 – 19)	11.3 (<0.1 – 153)	Reimann et al. (2014a)
GEMAS, EU, grazing land soil (0 – 10 cm)	<2 mm, total XRF (N = 2024)	<0.5 (<0.5 – 33)	<5 (<5 – 37)	n.d.	Reimann et al. (2014a)
USA, surface soil (0 - 5 cm)	<2 mm, total (ICP-MS[2], ICP-AES, N = 4857)	0.57 (<0.05 – 482)	0.8 (<0.1 – 1150)	20 (<1 – 300)	Smith et al. (2014)
USA, soil A-horizon	<2 mm, total (ICP-MS[2], ICP-AES[6], N = 4857)	0.57 (<0.05 – 630)	0.8 (<0.1 – 299)	20 (<1 – 514)	Smith et al. (2014)
Australia, NGSA[7], TOS[8] (0 - 10 cm)	<2 mm, AR[4] (ICP-MS[2], N = 1190)	0.12 (<0.02 – 18.1)	N/A[9] (<0.1 – 174)	N/A[9]	Caritat and Cooper (2011a, b)
Australia, NGSA[7], TOS[8] (0 - 10 cm)	<0.075 mm, AR[4] (ICP-MS[2], N = 1177)	0.15 (<0.02 – 27.1)	N/A[9] (<0.1 – >200)	N/A[9]	Caritat and Cooper (2011a, b)
Australia, NGSA[7], TOS[13] (0 - 10 cm)	<0.075 mm, HF+HNO$_3$ (ICP-MS[2], N = 1187)	N/A[9] (<0.4 – 28.9)	1.6 (<0.1 – 643)	N/A[9]	Caritat and Cooper (2011a, b)

Australia, NGSA[7], TOS[13] (0 - 10 cm)	<2mm, HF+HNO$_3$ (ICP-MS[2], N = 1190)	N/A[9] (<0.4 – 14.5)	1 (<0.1 – 327)	N/A[9]	Caritat and Cooper (2011a, b)
China, RGNRP[10], silt or fine sand on the drainage bottom, bank soil or dry stream sediment	<0.22 mm, total, (N = 1,568,528)	0.6 (<0.03 – 911)[11]	1.71 (<0.04 – 1073)[12]	31.1 (<0.4 – 560)	Xie et al. (2012)
BSS[14], agricultural soil (0 - 25 cm)	<2 mm, HF (ICP-MS[2], N = 747)	0.24 (<0.1 – 3.2)	N/A[9]	N/A[9]	Reimann et al. (2003)

[1] FOREGS - Forum of European Geological Surveys; [2] ICP-MS - Inductively Coupled Plasma Mass Spectrometry; [3] XRF - X-ray Fluorescence Spectrometry; [4] Stream sediment; [5] GEMAS - Geochemical Mapping of Agricultural and Grazing Land Soil in Europe; [6] ICP-AES - Inductively Coupled Plasma Atomic Emission Spectrometry; [7] NGSA – National Geochemical Survey of Australia; [8] TOS - top outlet sediment; [9] N/A – not available/applicable; [10] RGNRP – Regional Geochemistry National Reconnaissance Programme; [11] HG-AFS – Hydride Generation-Non-Dispersions Atomic Fluorescence Spectrometry; [12] POL – Polarography; [13] GF-AAS - Graphite Furnace Atomic Absorption Spectrometry; [14] BSS - Baltic Soil Survey: Agricultural Soils in Northern Europe. A Geochemical Atlas.

An explanation for the difference between UCC (total concentrations) and hot aqua regia results is that a major quantity of Sb occurs in minerals and phases which are not easily dissolved by acids. Sulphides, major host minerals for Sb, may not be very common in average soil. On the other hand, Sb can sorb onto Fe, Mn and Al oxides and hydroxides, clay minerals, and organic matter (Belzile et al., 2001; Buschmann and Sigg, 2004; Johnson et al., 2005), especially, when it occurs as oxyanions in low pH environments (Takahashi et al., 2010; Hockmann and Schulin, 2013). Some of the Sb can also be volatilised and lost during the hot acid extraction (Reimann et al., 2010).

The median Sb values and their concentration ranges in soil samples of different continental-scale surveys are provided in Table 2. The median Sb values vary between 0.12 mg/kg in Australia and 0.6 mg/kg in the European FOREGS topsoil. The Sb 'world soil' median of 1 mg/kg (with a range from <0.2 to 100 mg/kg), as provided by Bowen (1979), is about four times higher than the GEMAS hot aqua regia extractable Sb median. Kabata-Pendias and

283   Mukherjee (2007) provide better-constrained Sb concentrations with the background level of

284   Sb in topsoil samples between 0.05 and 4.0 mg/kg. Recently, the Sb data set of the LUCAS Soil

285   Survey (AR; ICP-AES; N=23,000; Cristache et al., 2014; ECS, 2010) published by Tóth et al.

286   (2016) reports values from 0.01 to 10.9 mg/kg with a calculated mean of 0.25 mg/kg. The

287   GEMAS median values for agricultural and grazing land soil samples (Reimann et al., 2014a,

288   b), based on 2108 samples, are thus comparable to those reported by the LUCAS project based

289   on over 23,000 samples. An advantage of the GEMAS results is that they are based on two

290   separately analysed and statistically treated land-use sample types (Ap and Gr) evenly covering

291   the whole survey area, while in the LUCAS project various land-use materials were analysed

292   and processed together. None of these different land-use classes provided an even coverage of

293   the European continent.

294   Some European regional geochemical surveys also provide Sb background data. In the

295   Baltic Soil Survey (Reimann et al., 2003), the median Sb concentration (HF extraction) is 0.24

296   mg/kg in TOP (0-25 cm) soil, which is nearly identical with the GEMAS median and its

297   concentration ranges between <0.1 and 3.2 mg/kg, while in the BOTtom (50-75 cm) soil it is

298   lower, 0.19 mg/kg (range: <0.1 – 1.41 mg/kg). The total Sb concentrations in topsoil samples

299   (0–15 cm) of England and Wales (Rawlins et al., 2012) range from 0.1 to 55 mg/kg, with a

300   median value of 0.7 mg/kg. In Irish topsoil (0–10 cm), the median value of Sb is 0.53 mg/kg

301   and the total concentrations vary from <0.05 to 5.29 mg/kg (Fay et al., 2007).
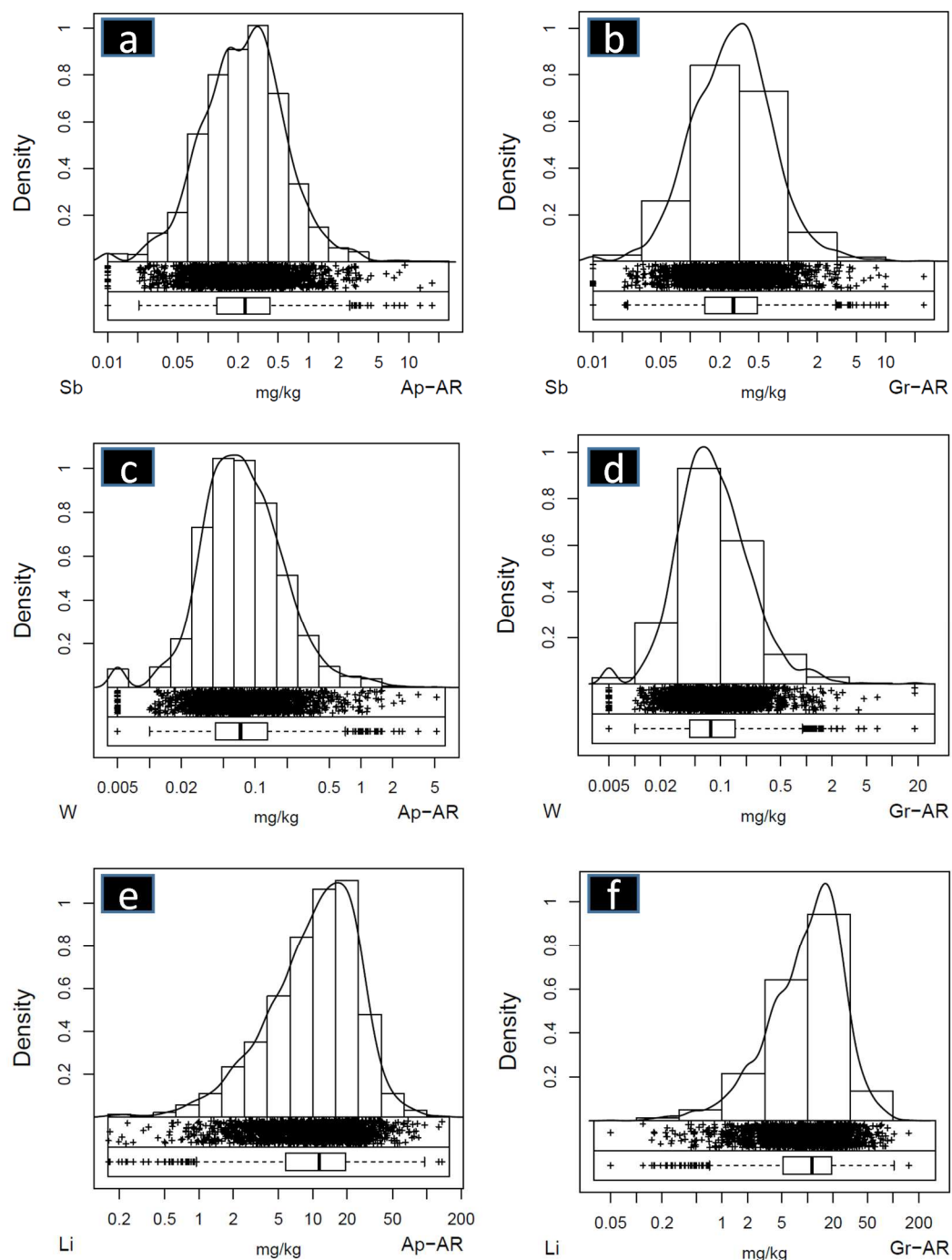
302

303

304

Figure 3. Combined plot of histogram, density trace, one-dimensional scattergram and boxplot
distribution in European Ap and Gr samples following a hot aqua regia extraction for the three
elements Sb (a for Ap and b for Gr samples), W (c for Ap and d for Gr samples), Li (e for Ap
and f for Gr samples).

3.1.2. W concentrations in agricultural soil

The median concentration of extractable W (aqua regia extraction) in the GEMAS

European soil is 0.073 mg/kg in the Ap and 0.077 mg/kg in the Gr samples. The combined plot

15

313 histogram - density trace one- dimensional scattergram - boxplot shows the univariate data

314 distribution of the aqua regia extractable W (Fig. 3c for Ap and 3d for Gr samples). The one-

315 dimensional scattergram and boxplot display the existence of upper and lower outliers in the W

316 distribution. The density trace, histogram and one-dimensional scattergram highlight the

317 samples below detection. The main body of the density trace and histogram exhibit an almost

318 symmetrical data distribution in the log-scale.

319   Because W does not substitute into most rock-forming minerals, its distribution in soil

320 is related largely to naturally occurring W mineralisation. Tungsten is enriched in mica (5–50

321 mg/kg), and muscovite in altered granite near W deposits may contain up to 500 mg/kg

322 (Wedepohl, 1978). A comparison of the GEMAS Ap soil W median to the upper continental

323 crust (UCC) estimated abundance of 1.9 mg/kg (Hu and Gao, 2008) shows that the hot aqua

324 regia extractable W is a factor of 27 lower in the European agricultural soil. Clearly, only a very

325 small percentage of total W in soil can be extracted by the mixture of HCl and HNO_3, even after

326 heating. XRF results for W in the GEMAS project vary around the method's detection limit,

327 but the interpretation of the data range and its maximum values indicates that the data set is

328 quite homogeneous, without many outliers. The extractability of W from the comparison of

329 aqua regia to XRF results is 3 and 4% for the Ap and Gr samples, respectively (Reimann et al.,

330 2011). The AR extraction is, therefore, not a sufficiently good method for extracting W from

331 soil samples, mainly because of the presence of resistant W-bearing minerals and precipitation

332 of insoluble tungstates and the polymerisation of tungstates onto soil particles (Bednar et al.,

333 2010).

334   Apart from the GEMAS project XRF results for W (Ap samples: <5 to 25 mg/kg, with

335 a median of <5 mg/kg; Gr samples: <5 to 37 mg/kg, with a median of <0.5 mg/kg), total W

336 concentrations, have been reported in three continental-scale soil geochemical projects, i.e., the

337 Geochemical Atlas of Europe (FOREGS; Salminen et al., 2005), the Geochemical and

338   Mineralogical Atlas of the Conterminous United States; Smith et al., 2014), and the

339   Geochemical Atlas of Australia (Caritat and Cooper, 2011a,b), all ranges and medians are

340   tabulated in Table 1. In the United States of America, the areas of very high total W values in

341   the Central and Southern Rocky Mountains are related to the Colorado Mineral Belt and the

342   Butte Mineral district in Montana (Smith et al., 2014). Mineral deposits enriched in W are

343   widespread throughout the western United States and are most often genetically related to

344   intrusions of felsic rocks.

345   In Europe, total W contents in the topsoil of England and Wales vary at the regional

346   scale from <0.6 to 70 mg/kg, with a median of 2.1 mg/kg (Rawlins et al., 2012). The anomalous

347   W concentrations in southern Devon and Cornwall are associated with mining and extraction

348   processes and occur around the granite intrusions of Dartmoor, Bodmin Moor and St. Austell.

349   In the Soil Geochemical Atlas of Ireland, W concentrations range between <0.1 and 7.72 mg/kg,

350   with a median of 0.59 mg/kg (Fay et al., 2007). High and elevated levels of total W are found

351   in soil developed on igneous rocks as well as on greywacke, black shale and fine-grained

352   sandstone (Fay et al., 2007).

353

354   3.1.3. Li concentrations in agricultural soil

355   The median concentration of Li in an aqua regia extraction in the GEMAS European

356   soil is 11.4 mg/kg in Ap and 11.3 mg/kg in Gr samples. The combined plot histogram - density

357   trace one - dimensional scattergram - boxplot displays the Li univariate data distribution in Ap

358   and Gr soil samples (Fig. 3e for Ap and 3f for Gr samples). One-dimensional scattergram and

359   boxplot highlight the existence of many outliers at the lower end of the Li distribution and very

360   few at the upper end. Though the density trace, histogram and boxplot suggest a slight skew,

361   the data distribution is still rather symmetrical in the log-scale, for both Ap and Gr types of soil.

362   During weathering processes, water-rock interaction and erosion, the geochemical behaviour

363 of Li is similar to that of Na, despite the difference in the abundance of both elements. However,

364 Li is more mobile in the surficial environment and during water–rock interactions. Owing to its

365 weaker binding than Na in ion exchange reactions, Li is preferentially leached during

366 weathering of silicate rocks. Lithium is very mobile during hypergenetic processes, as well as

367 in the initial stage of soil formation (Kabata-Pendias and Mukherjee, 2007). It may become

368 more stable due to its adsorption to clay minerals, Fe and Mn hydroxides, and organic matter

369 (Millot et al., 2010).

370 　　The comparison of Li to the estimated upper continental crust (UCC) abundance of 24

371 mg/kg (Hu and Gao, 2008) shows that the hot aqua regia extractable Li is almost a factor of 2

372 lower in the European agricultural soil samples. Large differences in the median values of Li in

373 GEMAS and in continental-scale geochemical soil surveys (Table 2) from China, U.S.A. and

374 Australia indicate that natural factors such as underlying geology, and technical aspects like

375 number of samples, sample size and methodology play a crucial role in data processing and

376 interpretation.

377

378 **3.2. Spatial distribution of Sb, W and Li in European soil and their source geology**

379 　　As very few differences are observed for the three elements between Ap (ploughing layer

380 of agricultural arable fields) and Gr (land under permanent grass cover) types of soil only the

381 data obtained for the Ap soil samples will be considered hereafter.

382 　　At first glance, geochemical maps for Sb, W and Li (Figs. 4b, 5b and 6b) reflect natural

383 sources of these elements and their spatial distribution seems to be governed by weathering type

384 and degree, Quaternary history, the underlying bedrock and mineralisation. The chemical

385 composition of soil represents largely the primary mineralogy of the source parent materials,

386 the effects of pre- and post-depositional chemical weathering, formation of secondary products

387 such as clays, and element mobility, either by leaching or mineral sorting. Geographical

388   distribution (based on ProMine Mineral Database, Cassard et al., 2012, 2015) of the mineralised

389   areas are shown in Figures 4a, 5a and 6a for Sb, W and Li, respectively, and the maps of Sb, W

390   and Li in the hot aqua regia extraction of agricultural soil samples are correspondingly displayed

391   in Figures 4b, 5b and 6b, respectively.

392

393   3.2.1. Spatial distribution of Sb

394   The Ap map of Sb in the hot aqua regia extraction show one of the most striking

395   differences in element concentration between the Ap soil of all analysed elements/parameters

396   (Fig. 4a) between northern (median 0.11 mg/kg) and southern Europe (median 0.35 mg/kg). It

397   is worth noting the difference in Sb concentrations between the upper continental crust and

398   world soil, 0.75 and 0.9 mg/kg, respectively, compared to values in Ap soil. This pronounced

399   disparity of Sb concentrations is most likely an effect of glaciation, soil age and weathering.

400   Soil pH is generally lower in northern than in southern Europe facilitating thus the removal and

401   accumulation of many elements including Sb from soil. Low pH and/or high content of organic

402   matter are two main factors controlling the fate of Sb in soil. Interestingly, Ap soil samples

403   collected in the far north over Archaean bedrock in Fennoscandia are characterised by the

404   lowest Sb contents in Europe, a feature also known from various local studies and national

405   geochemical surveys, e.g., Andersson et al. (2014). It seems, that soil developed on old cratonic

406   areas, such as the Fennoscandian Shield and East European Platform with the oldest bedrock in

407   Europe, are highly depleted in Sb in comparison with soil formed from parent materials

408   composed of younger bedrock in western and southern Europe. Even though Sb mineralisation

409   is usually located within granitic bodies, the pristine granitic massifs at several locations in

410   Europe show very low Sb contents in overlying soil, e.g., in NE Sardinia, northern Portugal and

411   western-central Spain (Fig. 4b). The enrichment in Sb occurs in soil developed on sedimentary

412   rocks such as shale, mudstone and young argillaceous rocks. Soil within the Carpathian Belt,

413 where flysch-type rocks dominate, has elevated Sb contents. More rarely, Sb can substitute Fe

414 and occurs as trace element in minerals typical of mafic rocks (e.g., in olivine) and, therefore,

415 certain Sb enrichment may occur in areas where mafic to intermediate volcanic rocks occur,

416 e.g., in Italy, France (Massif Central) and Czech Republic (part of the Bohemian Massif) exist.

417 A couple of Sb anomalies in Italy are associated with the Roman and Neapolitan alkaline

418 volcanic provinces (Nos. 36 & 37, Fig. 4b).

419 In the hypergene zone, Sb is often associated with Fe and Al oxides/hydroxides, and can

420 be sorbed onto silicate grains, representing a potentially bioavailable and extractable fraction

421 (Gal et al., 2007). Such a process may be possibly the cause of Sb enrichment in soil in warm
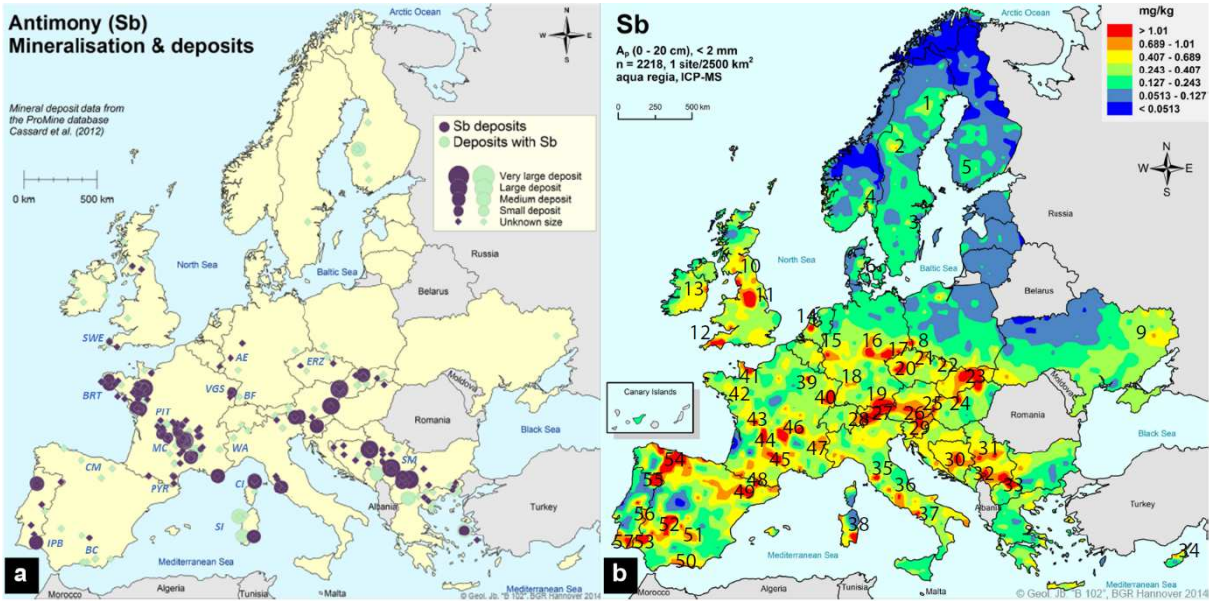
422 Mediterranean climates.

423

424 *Fig. 4. (a) Distribution of Sb-bearing ore deposits in Europe (based on the ProMine Mineral*
425 *Database; Cassard et al., 2012, 2015; Demetriades and Reimann, 2014). Abbreviations of*
426 *mineralised districts: AE: Ardennes–Eifel; BC: Betic Cordillera; BF: Black Forest; BRT:*
427 *Brittany; CI: Corsica; CM: Cantabrian Mts.; ERZ: Erzgebirge (Ore Mts.); IPB: Iberian Pyrite*
428 *Belt; MC: Massif Central; PIT: Poitou; PYR: Pyrenees; SI: Sardinia; SM: Serbo-Macedonian*
429 *ore district; SWE: South-west England ore district; VGS: Vosges; WA: Western Alps; (b) Soil*
430 *geochemical map for hot aqua regia extractable Sb concentrations in ploughed agricultural*
431 *soil (Ap, N=2108). Numbered anomalies are listed in Table 3.*

432

433 3.2.2. Spatial distribution of W

434   The geochemical map of W shows an interesting distribution pattern, which is different

435   from that of Sb (Fig. 5b). Though the northern European Ap soil displays somewhat lower W

436   values (median 0.058 mg/kg) than those from southern Europe (median 0.083 mg/kg), the

437   boundary does not exactly follow the limit of the last glaciation. This is due to the many high

438   values observed in German soil and, in general, in central Europe. In Germany, several

439   anomalies (from Hannover to the border of The Netherlands) coincide with the occurrence of

440   sedimentary iron ore deposits. Poland and Ukraine are in contrast marked by very low W

441   concentrations in Ap soil. This can be explained by the presence of aeolian deposits, coversands

442   and loess, deposited prior to, and just after, the last glaciation maximum and are of Weichselian

443   age (Zeeberg, 1998). These deposits are rich in Hf and Zr (Scheib et al., 2012) but depleted in

444   fine-grained fraction W, and the primary W minerals, such a scheelite and wolframite, are not

445   easily dissolved by traditional hot acid extractions. In fact, most of the elevated W background

446   in Europe is observed in areas underlain by crystalline bedrock.

447   Many granitic intrusions (see Fig. 5b; Cornwall in south-west England (No. 13),

448   northern Portugal (Nos. 49 & 50), Massif Central (No. 39) in France, for example) are clearly

449   marked by W anomalies, as are the Roman and Neapolitan alkaline volcanic rocks in Italy (No.

450   31). The Vosges (No. 38) and the Alpine region (especially the western part, Nos. 27, 28 & 29)

451   are marked by enhanced W concentrations. This is most likely related to the crystalline massifs

452   and to the extensive tectonic lines with associated magmatic rocks (Rhône-Simplon-Insubria-

453   Periadriatic Line) and metamorphic rocks (trace W concentrations are common in mica-rich

454   rocks). In Sweden and Finland, the predominance of granitic bedrock (Fennoscandian Shield)

455   over large parts of these countries is well reflected in somewhat enhanced W concentrations.

456   The higher nappes in the Scandinavian Caledonides (mainly calcareous sedimentary rocks) and

457   the Archaean bedrock in the north are characterised by low W soil concentrations. In eastern

458   Finland, W depletion delineates the location of so called greenstone belts. Generally, low W

459 contents in soil occur in areas with glacial drift (central Europe) and with transported calcareous

460 materials, e.g., in Denmark.

461   It is worth noting that the geochemical mobility of W is different from that of Sb; W is

462 mobile under oxidising conditions in alkaline waters and tends to adsorb to Mn-oxides, clay

463 minerals and binds to organic matter. Primary W exists almost exclusively in the form of

464 tungstate minerals (scheelite $CaWO_4$, wolframite $[Fe/Mn]WO_4$), which are resistant to

465 weathering. Under specific conditions, the formation of soluble W complexes, with many

466 inorganic and organic ligands, enhance its mobility in the surface and subsurface aquatic

467 environment (Koutsospyros et al., 2006).
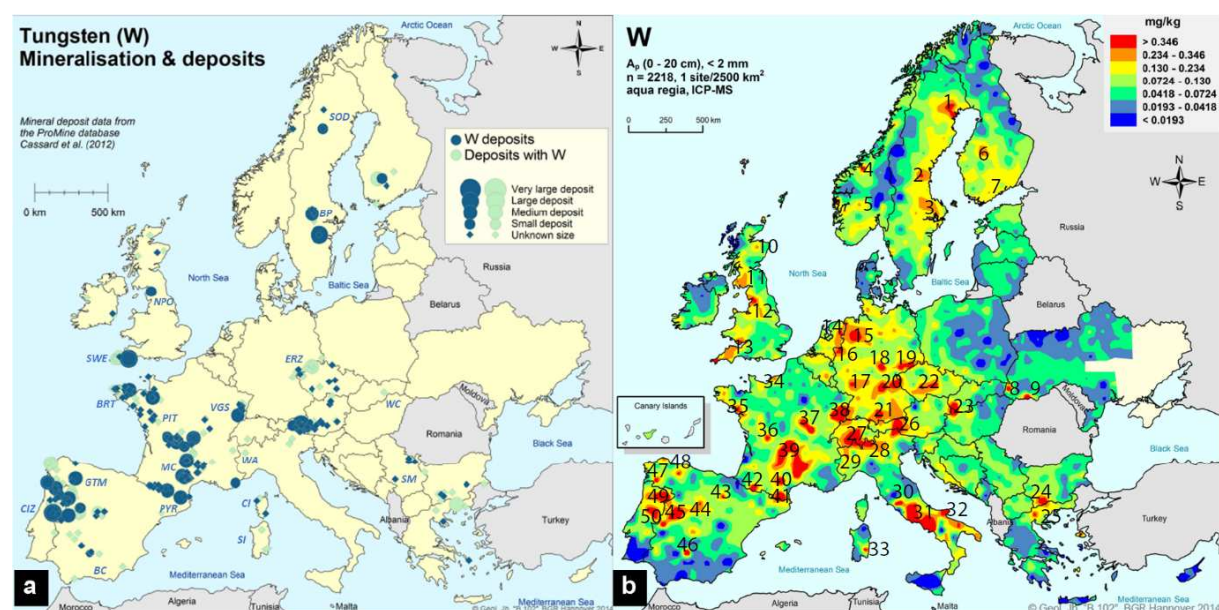
468

469

470 Fig. 5. (a) *Distribution of W-bearing ore deposits in Europe (based on the ProMine Mineral*
471 *Database; Cassard et al., 2012, 2015; Demetriades and Reimann, 2014). Abbreviations of*
472 *mineral districts: BC: Betic Cordillera; BP: Bergslagen ore province; BRT: Brittany; CI:*
473 *Corsica; CIZ: Central Iberian ore zone; ERZ: Erzgebirge (Ore Mts.); GTM: Galicia-Trás-os-*
474 *Montes zone; MC: Massif Central; NPO: North Pennine orefield; PIT: Poitou; PYR: Pyrenees;*
475 *SI: Sardinia; SM: Serbo-Macedonian ore district; SOD: Skellefte ore district; SWE: South-west*
476 *England ore district; VGS: Vosges; WA: Western Alps; WC:Western Carpathians (b) Soil*
477 *geochemical map for hot aqua regia extractable W concentrations in ploughed agricultural soil*
478 *(Ap, N=2108). Numbered anomalies are listed in Table 4.*

479

480

481   3.2.3. Spatial distribution of Li

482   The aqua regia extractable Li map displays typical GEMAS spatial distribution patterns

483   (observed for many elements), with predominantly low concentrations in Ap soil in northern

484   Europe (median 6.4 mg/kg Li) and evidently higher values in southern Europe (median 15

485   mg/kg Li; Fig. 6a). The maximum extent of the last glaciation is visible as a discrete

486   concentration break on the Ap geochemical map of Li (Fig. 6b). The principal Li anomalies are

487   spatially associated with granitic rocks throughout Europe, e.g., northern Portugal (Nos. 46,

488   47), Massif Central (Nos. 37 & 38) in France, Wales (No. 10), south-west England (No. 11).

489   While in Fennoscandia the Central Scandinavian Clay Belt (Ladenberger et al., 2014) is clearly

490   visible (Nos. 3 & 5), and this feature emphasises the tendency of Li to bind to clay (although

491   developed on the crystalline, mainly granitic bedrock). The Alpine Region (especially the

492   western part) is marked by enhanced Li concentrations (Nos. 26 & 30). This is most likely

493   related to the crystalline massifs and to the extensive tectonic lines with associated magmatic

494   rocks (Rhône-Simplon-Insubria-Periadriatic Line). In northern Portugal, the extensive Li

495   anomaly (Nos. 46 & 47, Fig. 6b) is related to the occurrence of Li-pegmatites. The anomaly in

496   the Wolfsberg area in Austria (No. 26) is also associated with Li-pegmatites with no known

497   relation to any granite. High Li values occurring over karst limestone areas in southern Europe

498   (Croatia, No. 22) are possibly due to secondary Li enrichment attributed to climatic conditions,

499   and to phosphorite and bauxite occurrences (Hellas, Nos. 24 & 25). In arid areas, Li can be

500   enriched via precipitation (together with other evaporite minerals). Lithium's tendency to bind

501   to clay leads to enrichment in fine-grained sedimentary rocks, both young and unaltered and

502   those metamorphosed into schist. Additionally, Li occurs in trace amounts in mica and

503   amphibole minerals, and soil with mica-rich parent materials (such as mica schist) can have

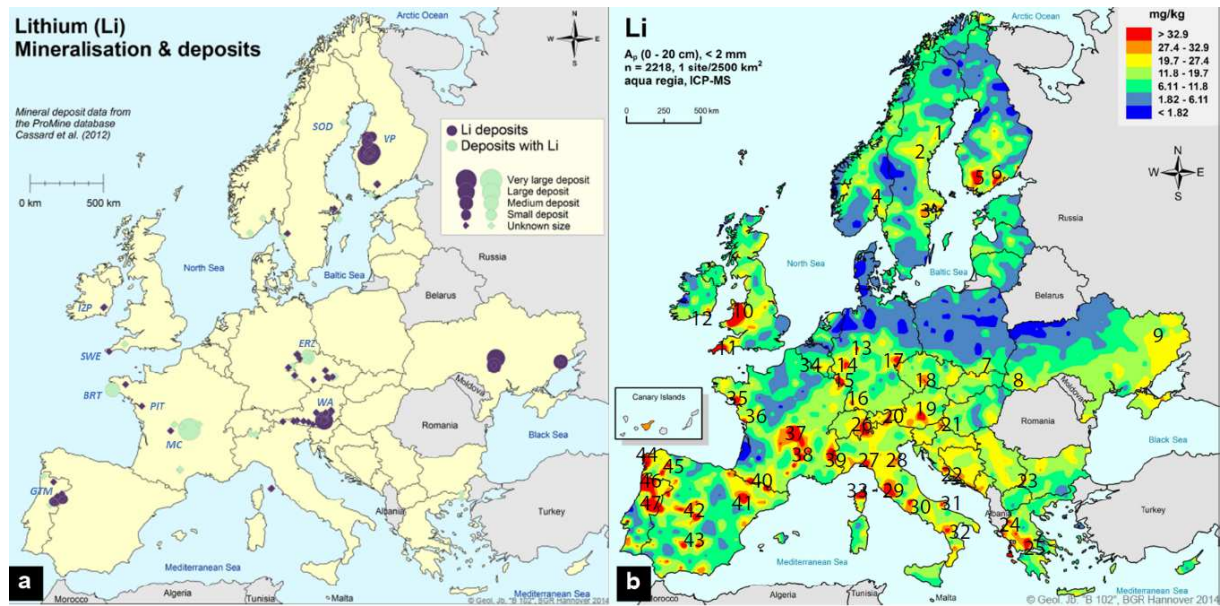504   high Li concentrations.

Fig. 6. *(a) Distribution of Li-bearing ore deposits in Europe (based on the ProMine Mineral Database; Cassard et al., 2012, 2015; Demetriades and Reimann, 2014). Abbreviations of mineral districts: BRT: Brittany; ERZ: Erzebirge (Ore Mts.); GTM: Galicia-Trás-os-Montes zone; IZP: Irish Zn–Pb ore district; MC: Massif Central; PIT: Poitou; SOD: Skellefte ore district; SWE: South-west England ore district; VP: Vihanti–Pyhäsalmi ore district; WA: Western Alps. (b) Soil geochemical maps for hot aqua regia extractable Li concentrations in ploughed agricultural soils (Ap, N=2108). Numbered anomalies are listed in Table 5.*

The Li concentration is compared with the clay content in Fig. 7. The classical representation of Li concentration (mg/kg) *vs.* clay content (%) evidenced the existence of heteroscedasticity in the data. To overcome this, the Li concentrations are plotted with logarithmic scaling and the clay contents are expressed as a binary logit function, i.e., a logistic transformation according to log[P/(100-P)] where P is the clay content. A clear trend is observed in Figure 7, less visible, however, for soil developed on coarse-grained sandy deposits ('quartz') and calcareous rock ('chalk'), since these parental materials do not produce clay minerals under weathering processes. Better correlation occurs in soil developed on greenstone ('green') and Precambrian bedrock (granitic gneiss - 'prec') – these parent materials are sources to thick clay overburden as a result of weathering, especially in warm and humid climate.

The correlation between Li and Fe and Al was earlier reported by Reimann et al. (2012a). The strong Li-Al correlation can be explained by the fact that kaolinite, the most

24

526   aluminous mineral, easily fixes large amounts of Li compared to other minerals such as illite or

527   chlorite (Tardy et al., 1972). Using a selection of regional data from the GEMAS project (e.g.,

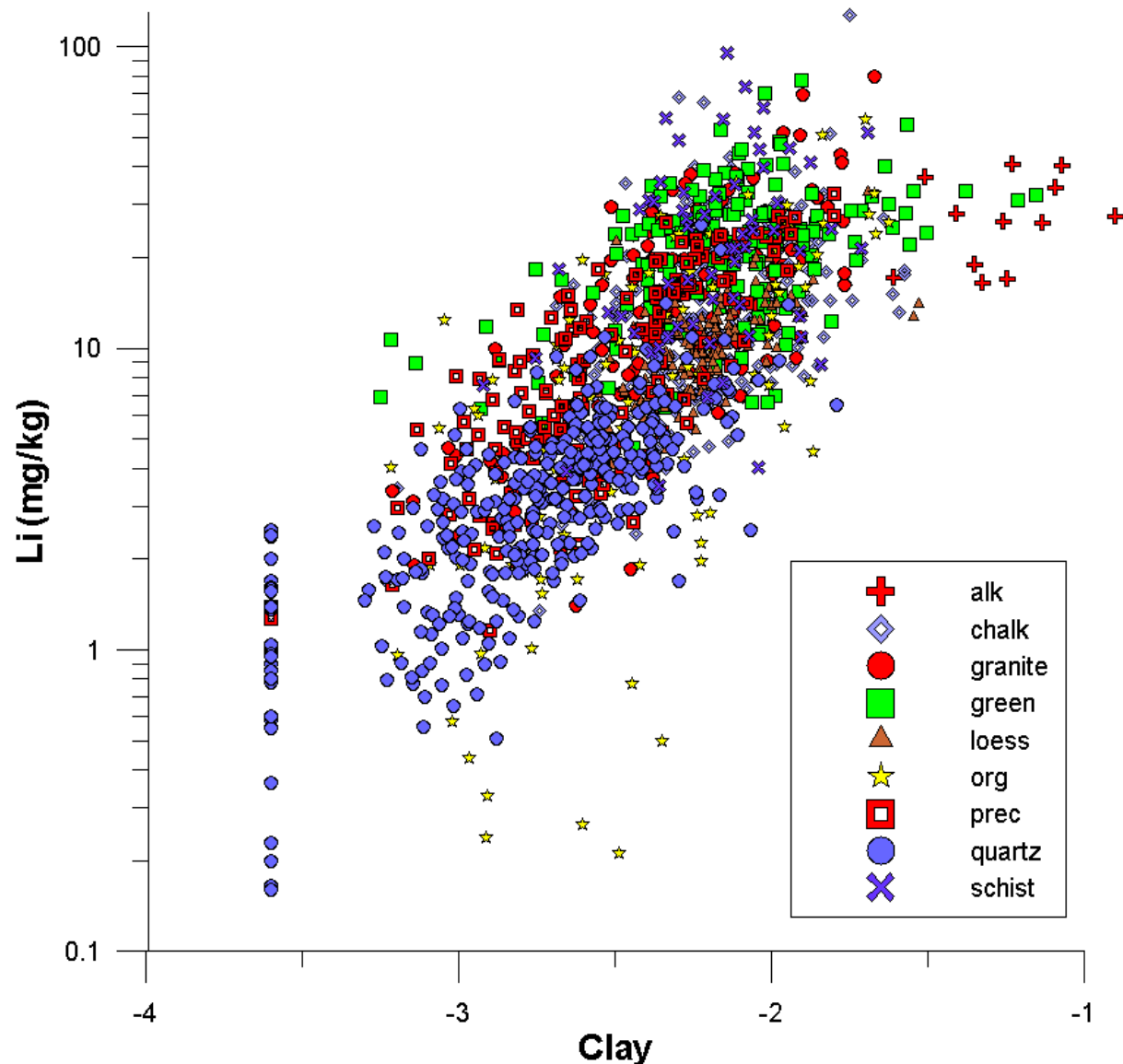528   from Nordic countries), this very strong relationship between Li and Al is shown (Fig. 8).

529

530   *Fig. 7. Plot of clay (%) and Li (mg/kg) contents in European Ap soil samples. Data are*
531   *classified according to the ten geological parent material subgroups (Reimann, 2012a, b),*
532   *comprising alk: alkaline rock; chalk: calcareous rock; granite: granitic bedrock; green:*
533   *greenstone, basalt, mafic bedrocks; loess: loess; org: organic soil; other: unclassified bedrock;*
534   *prec: predominantly Precambrian granitic-gneiss; quartz: soil developed on coarse-grained*
535   *sandy deposits; schist: schist.; the category 'other' in the original classification has not been*
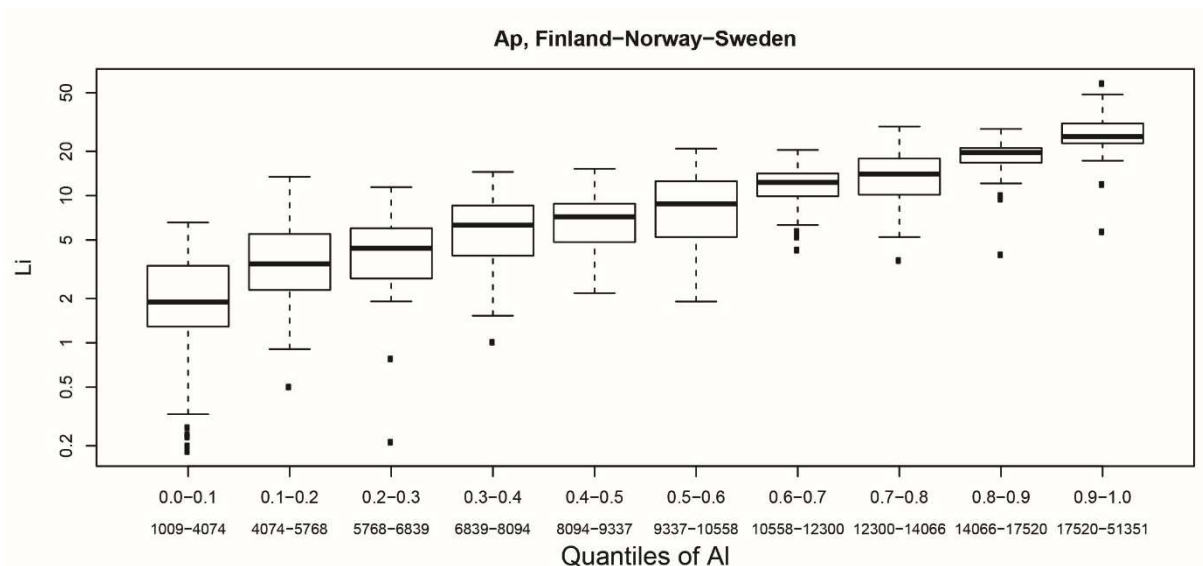536   *plotted on the graph.*
537

Ap, Finland–Norway–Sweden

Fig. 8. Multiple boxplots showing relationship between Li concentrations (mg/kg) and Al quantiles in Ap GEMAS samples from Sweden, Finland and Norway (Ladenberger et al., 2013).

3.3. Emerging critical elements in soil as mineral potential indicators

Nowadays, high-tech elements are rarely mined as a main ore. Most often, they are co-products from the principle ore (e.g., Zn, Fe, Cu). In order to identify economic resources of high-tech materials, Sb, W and Li from agricultural soil (Ap) are used as proxies, and it is here discussed whether the geochemical anomalies in soil can be utilised for mineral exploration purposes. It is vitally important to be able to discriminate 'real' anomalies, high element concentrations related to potential economic mineralisation, from secondary enrichment caused by weathering, climate, contamination, etc. Historical and inactive mining regions can be of interest since there are a strong political and environmental reasons to utilise mining wastes, such as tailings and waste heaps.

The majority of Sb, W and Li GEMAS geochemical anomalies in Ap soil can be directly related to known mineralisation and ore deposits (Figs. 4 to 6 and Tables 3 to 5). Except for deposits in the Fennoscandian Shield, most of the ore deposits in Europe are located within Palaeozoic to Caenozoic tectonic units and are related to respective orogenic events, e.g., in the Ordovician (Caledonian orogeny), Carboniferous (Variscan orogeny) and Tertiary (Alpine

Orogeny). Active volcanism, regional metamorphism and hydrothermal activity often accompanied these events. In western, central and southern Europe, most mineralisation is located in Variscan and Alpine units, while within the Fennoscandian Shield in northern Europe the majority occurs in Proterozoic (Sweden, Finland) and Caledonian (Sweden and Norway) terranes.

In order to evaluate the mineral potential of Sb, W and Li, GEMAS maps have been compared to the ProMine Mineral Database and European Minerals Knowledge Data Platform (Cassard et al., 2012, 2015, which is based on the ProMine Mineral Database; http://minerals4eu.brgm-rec.fr/) (Tables 3 to 5). These online databases contain compiled information about mineralisation and ore deposits for Europe and are often used by companies and policy makers. While most mineralisation is not reflected in the Ap soil geochemistry, there are several relatively large anomalies which cannot be easily explained by the ProMine Mineral Database. Such an example is Sb anomaly No. 39 in eastern France, which coincides with a Pb anomaly (No. 22 in Reimann et al., 2012b) where there is no known mineralisation, no smelter, no major city but correlate well with the proximity to Verdun, a small city made famous because of a fierce First World War (WW1) battle. Anomalies of Sb (No. 49) and Li (No. 41) are also unexplained by the ProMine Mineral Database and they appear to be significant in northern Spain. These geochemical anomalies can be found in the Geochemical Atlas of Spain (Locutura et al., 2012) and they seem to correlate with known polymetallic mineralisation (Pb-Zn-Cu-Ag-Sb-Bi-As-W-Au) in the pre-Pyrenean and Pyrenean region and to the existence of clays and evaporitic salts north of Zaragoza city and 100 km east in the Cardona-Suria Salt mines.

Interestingly, many anomalies of Sb, W and Li can be correlated to the ProMine Mineral Database deposits, which do not list these particular elements as associated commodities, e.g., Nordli Mo deposit in Norway and base-metal sulphide deposits in northern Sweden (Skellefte district). Additionally, a difference in background concentrations between northern and

581 southern Europe requires a separate interpretation of Fennoscandian countries by taking into

582 account the local background levels.

583

584 *Table 3. Explanation of Sb anomalies in Europe: comparison with ProMine Mineral*
585 *Database (PMD; Cassard et al., 2012, 2015). For anomaly numbers see Fig. 4a.*
586

No.	Country	Explanation (PMD)	Other explanation
1	Sweden (N Sweden)	Various sulphide deposits with Zn, Ag, Au, Cu, Pb	Skellefte Ore District
2	Sweden Central Sweden)	Zn-Cu-Pb deposits	Black shale in the Lower Allochthon in the Caledonides
3	Sweden (SE Sweden)	Associated with Zn-Pb and W mineralisation (associated with Mo and Sb)	
4	Norway (S Norway)	Sulphide mineralisation in volcanic rocks of the Oslo Rift, Cu-Mo and Au deposits	
5	Finland (S Finland)	Au deposits associated with Ag, Cu, Bi and Sb	
6	Denmark, (E Jutland)	Fe mineralisation in young postglacial sediments	
7	Poland (central-northern Poland)	Lignite deposits (Miocene) or sedimentary Fe deposits (Jurassic)	
8	SW Poland/SE Germany	Lignite deposits (active opencast mines)	Former lignite power plants and ash dumps, old opencast lignite mines
9	Ukraine	Hg deposits associated with silicified sandstone and coal (Donbass region	
10	United Kingdom (Scotland)	Various sulphide mineralisation with Sb, associated with Cu, Mo, Au and Ag; Coalfield region.	
11	United Kingdom (Bradford-Manchester)	Old mining region with Pb deposits, sphalerite, pyrite, galena, chalcopyrite, F and Ba. Coalfield region	
12	United Kingdom (Cornwall)	Sb sulphide mineralisation, associated also with Pb, W and Sn. Fault-related vein deposits	
13	Eastern Ireland	Sulphide deposits with Zn, Au, Cu, Pb and Sb, e.g., in Glendalough, Wicklow and Avoca region)	Possible contribution of contamination from the capital city of Dublin
14	Netherlands (Amsterdam)		Anthropogenic anomaly related to Amsterdam city

No.	Country	Explanation (PMD)	Other explanation
15	Germany (Rhenish Slate Mts, Nordrhein-Westfalen, Rheinland-Pfalz	Sb sulphide deposits, limonite occurrences and historical smelting	Pb-Zn-(Ag) sulphide deposits in the Stolberger mining district
16	Central Germany (Mansfeld, Lutherstadt Eisleben, Gräfenroda)	Northern anomaly: Cu Kupferschiefer deposits; Pb smelter	Southern anomaly: Thuringian Forest, Cu-Pb-Zn-Ag mineralisation following the Hercynian Eichenberg-Gotha-Saalfelder fault zone; Copper shale deposits (abandoned Cu mines and mining heaps)
17	Germany (Erzgebirge, East Thuringian Slate Mts)	Polymetallic vein mineralisation Bi-Co-Ni-Ag-U, arsenides	Eastern Ore Mts.: Sn deposits, Altenberger ore district, Schellerhauer granite; Western Ore Mts.: Kirchberger granite, W-Mo mineralisation, hard coal deposits near Oelsnitz; Sb-(Ag-Pb-Fe-As) mineralisations in the Berga Antiform
18	SW Germany (Karlsruhe-Stuttgart region; Pforzheim in Schwarzwald)	Open pit mining with fluorite associated by Bi and Cu in vein and breccia deposits	
19	S Germany - W Austria (Insbruck region)	Leogang (inactive plant) with Fe, Mn, Co, Ag, Cd, Hg, Ga, In, Ge, Sn, Sb	
20	Czech Republic (Plzen)	Coal and lignite deposits with Ge (Plzen and Radnice basin); Sb (antimonite)-Zn-Pb deposits	
21	Czech Republic/ Poland	Fe deposits with Sb; coal deposits	
22	Czech Republic (Opava)	Pb mineralisation; minor coal deposits	
23	Central Slovakia	Numerous Sb deposits (with Sb, Pb, Zn, Ag and Au)	Few localities with larger findings of Sb minerals, together with Au and Ag in hydrothermally altered Miocene andesites - www.mindat.org)
24	Hungary (N of Budapest, Visegrad)	Pb-Zn mineralisation	Anthropogenic anomaly – Budapest City

No.	Country	Explanation (PMD)	Other explanation
25	E Austria/W Hungary	Sb-Hg mineralisation; lignite deposits	
26	S Austria	Carbonate-hosted Pb-Zn deposits (MVT) with Ga, Ge, Pb, Zn; Cu VMS deposits; inactive plants (mainly surface storage)	
27	W Austria (Insbruck)	Pb-Zn deposits; skarn deposits with W; Cu deposits; inactive plants (mainly surface storage)	
28	W Austria/N Italy	Minor Zn mineralisation (with Ga and In); inactive plants (mainly surface storage)	
29	Slovenia	Sb mineralisation (vein and disseminated); Pb-Zn carbonate-hosted deposits (MVT)	
30	Bosnia & Herzegovina (Sarajevo region)	Sb mineralisation; Pb-Zn mineralisation; open pit mining (Pb-Zn with Sb)	
31	Serbia	Cu-Au VMS deposits; Sb vein deposit; Sediment-hosted precious metal deposits	
32	S Serbia	Sediment-hosted precious metal deposits with Sb; Pb-Zn Sedex deposits; coal deposits	
33	SE Serbia/ North Macedonia	Sb deposits; Pb-Zn +Ag skarn mineralisation; Sb deposits with stibnite	
34	N Cyprus		Western part of the Kyrenia Terrain (Alpine orogenic belt); however, it is most likely a transported anomaly, and related to the Troodos Ophiolite complex massive sulphide mineralisation; it correlates with anomalous Ag, Au, As, Hg, Pb, S, V and Zn
35	Central Italy	Sb deposits	
36	Central Italy	Sediment-hosted Sb mineralisation, related to shallow intrusions	Rome – anthropogenic anomaly; young volcanic rocks in the Rome region
37	S Italy (Naples)		Naples anthropogenic anomaly; young volcanic rocks (Vesuvius) which are responsible for Sb enrichment in local soil and groundwater

No.	Country	Explanation (PMD)	Other explanation
38	SE Sardinia (Italy)	VMS deposit with Sb (antimonite); Pb-Zn deposits, Ag-Sb mineralisation, Zn-Sb carbonate-hosted stratabound and vein mineralisation (MVT)	
39	E France	anthropogenic	Verdun – WW1
40	E France (Vosges)	Sb mineralisation; Pb-Cu-Ag mineralisation	Similar anomaly is observed for Pb (Reimann et al., 2012b); Variscan orogen
41	N France	Sediment-hosted baryte-Sb deposits, vein and metasomatic polymetallic deposits with Sb, Cu, Pb	
42	NW France	Polymetallic, mainly vein types deposits with Sb, Bi, Mo, Sn, W in granitic host rocks	
43	W France	Carbonate-hosted (in karst) Pb-Zn (+Ag) deposits MVT, known since medieval time; historical Ag smelting	
44	France (Limoges, Haute-Vienne, W Massif Central)	Carbonate-hosted Pb-Zn (Ag) MVT deposits; several Sb mineralisation with stibnite and berthierine, related to numerous Au deposits	Au-bearing granitic mica schist
45	France (S Massif Central)	Pb-Zn (Ag) deposits; Sb mineralisation with stibnite, a large system of Au and sulphide-rich quartz veins	
46	France (Massif Central, S of Clermont Ferrand, and west of Lyon)	Numerous Sb mineralisation associated with Au, Ag, Pb, Zn; mainly fault-related	
47	SE France (Grenoble)	Cu-Pb-Ag + Au (±Sb) fault related deposits, sandstone ± dolomite hosted Pb-Zn + Ag +Sb deposits	
48	NE Spain/Andorra (Pyrenes)	Volcano-sedimentary Zn-Ag deposits	
49	NE Spain (S Pyrenes)		Various polymetallic mineralisation (Pb-Zn-Cu-Ag-Sb-Bi-As-W-Au) in the pre-Pyrenean and Pyrenean region (Locutura et al., 2012)

No.	Country	Explanation (PMD)	Other explanation
50	S coast of Spain (Granada region)	Fault-related vein and breccia deposits with Ag, Zn (galena); vein and disseminated Sb deposit; carbonate-hosted Pb-Zn deposits with Ag	
51	Central Spain	Sb vein deposits; fault-related Pb-Zn-Ag deposits	
52	Central Spain (N of Cordoba)	Pb-Zn-Ag deposits (with galena, sphalerite)	
53	SW Spain	Iberian Pyrite Belt: Zn-Pb-Cu (+Ag) VMS deposits	
54	NW Spain (Galicia, Oviedo region)	Coal deposits; numerous Au deposits (quartz veins, conglomerate and alluvial placer); Sb (stibnite) deposits with cinnabar	
55	NE Portugal	Au-As mesothermal deposits (Au, Ag, As, Zn, Pb); Sn-W deposits (cassiterite, wolframite, scheelite, silver, pyrite, arsenopyrite, marcasite) in granitic veins and stockworks (greisen)	
56	Central Portugal	Sb-W fault-related deposits; Au-Sb mineralisation	
57	S Portugal	Sb fault-related deposits (antimonite, malachite, baryte, silver); Zn-Pb-Cu (+Ag) VMS deposits	

587

3.3.1. Antimony in soil as a mineral potential indicator

589

590   By studying the Sb maps in more detail (Figs. 4a, b), it can be observed that most of the

591   identified anomalies correspond with known mineral belts or ore deposits (Table 3). The highest

592   Sb contents in Ap soil occur in Portugal where several known Sb occurrences are located, for

593   example, within the so called Iberian Pyrite Belt, in south-eastern Portugal. In Austria, an Sb

594   anomalous region stretches in a form of a belt in the Alps and coincides with many known

595   mineralised occurrences and historical mines. The Massif Central in France with its extensive

596   hydrothermal mineralisation stands out as an anomaly, as does the Iberian Pyrite Belt (southern

597   Spain and Portugal), the Vosges (French and German border), Ardennes-Eifel (Germany), the

598 Ore Mountains (German and Czech border), Bohemian Forest (Czech Republic), Carpathians

599 (Slovakia), and the Pennine and south-west England ore-fields in the United Kingdom. High

600 Sb contents in Ap soil occur also in the Balkan countries, Bosnia and Herzegovina, Serbia (with

601 Kosovo), North Macedonia and Hellas, and they all are related to various types of

602 mineralisation, mainly polymetallic with Pb-Zn-Cu, the Serbo-Macedonian mineralised zone.

603   Due to strong contrast in Sb concentrations between northern and southern Europe, the

604 Sb concentrations in the soil of Fennoscandia, Estonia, Latvia, Lithuania, northern Poland,

605 Denmark and northern Germany should be displayed as a separate data set (Fig. 9). In

606 Fennoscandia, relatively high Sb concentrations are mainly related to polymetallic

607 mineralisation, e.g., Pb-Zn-As deposits in northern Sweden (Skellefte district), Sb, Bi, Au and

608 As mineralisation north-west of Luleå, and in central Sweden (Bergslagen district). Known Zn-

609 Pb mineralised occurrences in SW Scania in southern Sweden are indicated by a large Sb

610 geochemical anomaly in grazing land soil. High Sb concentrations in two Ap soil samples are

611 unexplained; one in the northernmost Sweden within the Archaean bedrock and the other in SE

612 Sweden (Småland, near Oskarshamn). The remarkable enrichment in Sb in the fine-grained

613 sedimentary rocks (mainly in black shale, e.g., in the Lower Allochthon of the Caledonides),

614 although appearing very promising, has potentially no economic significance mainly because

615 Sb is dispersed at low levels and does not form economic ore-bodies, as its mining is difficult

616 and requires processing of large volumes of rocks. In Norway, large Sb anomalies are closely

617 related to mineralisation within the Oslo Rift and in SW Norway with some sulphide
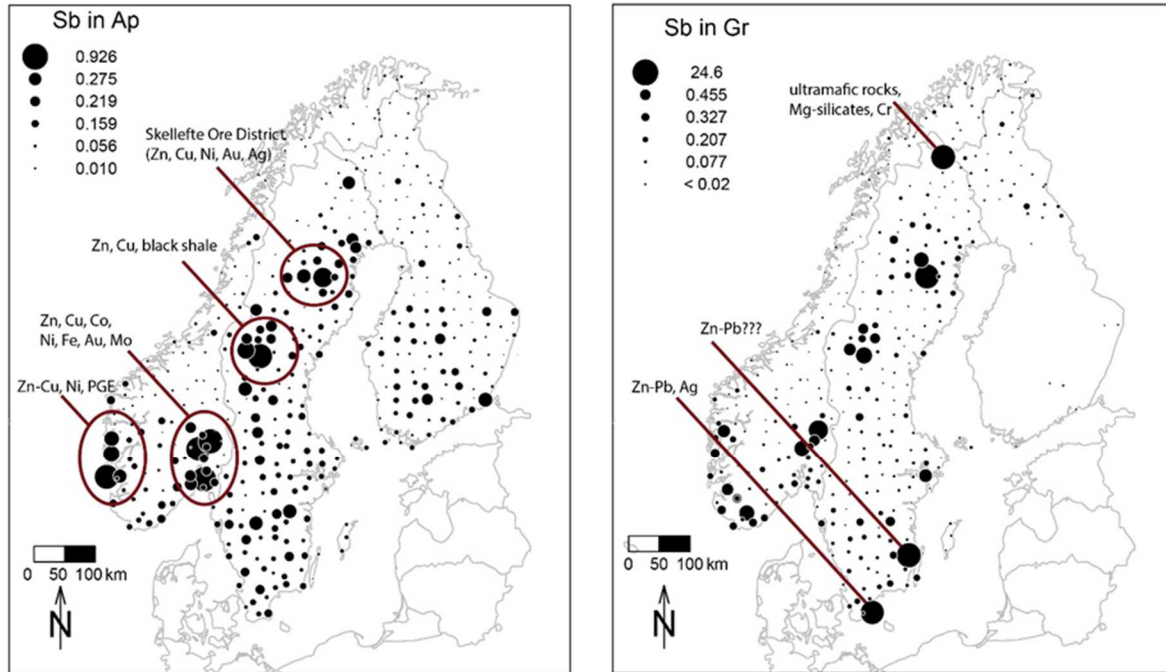
618 polymetallic deposits (Fig. 9).

Fig. 9. Sb geochemical maps (mg/kg) in Ap (n=453) and Gr (n=350) soil of Norway, Sweden and Finland. Regional Fennoscandian percentile calculation allows clear detection of anomalies. Most of them can be explained by mineralisation or lithology.

Economic occurrences of Sb in Europe are mainly associated with sulphide deposits, and Sb can be used as a pathfinder element for sulphide mineral deposits (Boyle, 1974; Boyle and Jonasson, 1984). Another example is from deposits in Austria that were economic in their time related to their mono-mineral characteristic (stibnite). Antimony is also used together with As and Bi as a pathfinder element for Au mineralisation (Boyle, 1974; Boyle and Jonasson, 1984; Plant et al., 1989). In other words, using Sb, sulphide ores can be classified according to their potential for hosting by-products of economic importance.

Because many of the Sb-hosting deposits have been mined historically (e.g., in France), it is difficult to evaluate to what extent Sb anomalies are natural anomalies (due to the occurrence of the deposits themselves) or whether the extent of mining and smelting activities has accentuated originally very local anomalies. To answer the question 'natural or anthropogenic' in these areas, detailed studies would be needed in every single case. On the other hand, the size of an anomaly can be used as pathfinder for potential future recovery at the

34

source (e.g., from past tailings). Otherwise, typical anthropogenic Sb anomalies related to urbanisation, although rare, they have been recognised near Amsterdam, Budapest, Rome and Naples. Additionally, interesting historical Sb impacts can be observed, e.g., in Naples region (Italy). The rather large Sb anomaly, apart from possibly being anthropogenic (Naples), coincides with the location of Europe's largest volcano – Vesuvius. Antimony occurs naturally in groundwater close to volcanoes, and Pompeii's proximity to Mount Vesuvius could have provided Sb concentrations in the water that were even higher than in a typical Roman city at the time. Antimony poisoning is known in this area from historical times. The Pb pipes in Pompeii, studied by archaeologists, contain Sb which was likely a cause of health problems among the residents (Charlier et al., 2017).

Table 4. Explanation of W anomalies in Europe: comparison with ProMine Mineral Database (PMD; Cassard et al., 2012, 2015). For anomaly numbers see Fig. 5.

No.	Country	Explanation (PMD)	Other explanation
1	N Sweden	Cu-Ag mineralisation with scheelite occurrences	W mineralisation in skarn; associated Cu, Zn, Au, Ag mineralisation (SGU database)
2	Central Sweden	Au-Cu+Ag mineralisation	Many small W mineralised occurrences and historical W (+Pb+Cu) mining (SGU database)
3	Central Sweden (Bergslagen)	Scheelite mineralisation (+Mo, Fe-Cu-Ag) and historical mining sites	
4	W Norway (Molde-Ålesund)		Mineralisation in quartz-rich lithologies, V-Fe-Ti mineralisation in western Norway (FODD database)
5	S Norway (Bergen, Odda)		Small granitic intrusions, Zn-Cu-Au mineralisation (source: FODD database); Odda - a major Zn smelter in Norway
6	Central Finland	Mineralisation in pegmatites, numerous gold occurrences	
7	S Finland	Scheelite-Mo (As+Co) skarn mineralisation, associated Au mineralisation	
8	SW Ukraine		Epithermal polymetallic deposits in Transcarpathian region. Vein-

No.	Country	Explanation (PMD)	Other explanation
			type Au-base metal deposits hosted by volcano-sedimentary sequences of the Pannonian basin in the Carpathian Neogene volcanic belt
9	SW Ukraine		Au-Ag-Zn-Pb-Cu mineralisation and epithermal deposits in Transcarpathian region
10	Scotland	Wolframite-scheelite mineralisation in Devonian granites (associated with cassiterite, molybdenite, sphalerite, chalcopyrite, topaz)	
11	Scotland W (Southern Uplands)	Au-Pb-Cu-As-Ag mineralisation	
12	NW England (southern part of Lake District and Pennines)		W mineralisation in the Lake District (Cumbria)
13	United Kingdom (SE Wales, Cornwall)	Wolframite-cassiterite mineralisation (Cs+Li) in Cornubian orefield	W mineralisation in Cornubian batholith
14	NE Netherlands	unexplained	
15	NW Germany (Lower Saxony)	Fe-Ag-Pb-Zn mineralisation in felsic alkaline plutonic rocks; metasomatic carbonate-hosted haematite-magnesite deposits; Fe smelter	Abandoned iron ore mines
16	W Germany (North Rhine-Westphalia)	Fe smelter	Hard coal deposits and mining, inactive hard coal power plants
17	Rhineland-Palatinate	Minor Ag-Cu mineralisation	Donnersberg rhyolite massif, historical Cu mines
18	Central Germany (Thuringian Forest)	Cu-Pb-Zn-Ag mineralisations	Cu-Pb-Zn-Ag vein mineralisation following the Hercynian Eichenberg-Gotha-Saalfeld fault zone; Cu shale deposit
19	SE Germany (Erzgebirge, Ore Mts)	Sn-W (+Ag+Zn+Ge) mineralisation in greisen	W-Mo mineralisation in the area of Kirchberger granite
20	S Germany (W and NE Nürnberg) / W Czech Republic	U-W (+Sn) mineralisation	Pb-Zn mineralisation, Baryte-fluorspar-haematite mineralisation

No.	Country	Explanation (PMD)	Other explanation
21	S Germany (Molasse basin)	Minor Pb-Zn mineralisation	Pitch coal occurrences (strong pressed lignite) in the south
22	Central Czech Republic	W and Pb-Ag mineralisation	
23	SW Slovakia-NW Hungary	Au-Sb-Ag-Zn-Pb mineralisation	
24	SW Bulgaria (Western Rhodopes Mts)	polymetallic W-Bi-Mo deposits; W-Pb-Mo-Cu mineralisation in granite and skarn	
25	Hellas (Central Macedonia)	Sb-W vein mineralisation; Cu-Ag-Au porphyry deposits	
26	W Austria (Insbruck, Hohe Tauern)	Numerous W occurrences (scheelite-Mo skarn)	
27	S Switzerland	Au, REE, Pb-Ag-Zn mineralisation	
28	N Italy	Zn-Ag carbonate-hosted mineralisation	
29	NW Italy	Cu-Ag mineralisation	
30	Central Italy	Minor Sb (Hg, Cu, Zn, Pb) mineralisation	Volcanic origin
31	Central Italy (Rome-Naples region)		Volcanic origin
32	Italy (Gargano Peninsula)		Plutonic and volcanic alkaline rocks (gabbro and syenite, anorogenic lamprophyres); skarn mineralisation at the contact with limestone
33	SE Sardinia	W-Zn-Pb mineralisation; Mo-W mineralisation in greisen; Sb-W VMS deposits; Au mineralisation; Ag-Sb-Pb-Zn polymetallic veins	
34	N France	unexplained	
35	NW France	W (scheelite) – Mo skarn mineralisation; wolframite in greisen	
36	W central France (Poitu, Limousin, Haute-Vienne)	Numerous W (+Mo, Sn, Zn, Cu) mineralised occurrences in relation to granitic intrusions and in greisen	
37	Central France	W (+Sn, Mo, Py) mineralisation in granite and greisen	

No.	Country	Explanation (PMD)	Other explanation
38	E France (Vosges)	Numerous W mineralisation; W-Mo skarn; wolframite and scheelite in greisen	
39	Central France (Massif Central)	Numerous W mineralisation (+Bi, Sn, As, Mo, Cu)	
40	S France (Provence-Alpes-Côte d'Azur region)	Numerous W mineralisation, carbonate hosted Pb-Zn MVT deposits; W-Mo skarn deposits in greisen (with Sn)	
41	S France (Pyrenees)	W-Mo skarn mineralisation, associated with Au and Ag	
42	S France (Pyrenees)	W-Mo skarn mineralisation, associated with Ag, Zn and Pb	
43	N Spain	Minor Ag occurrences	
44	Central Spain, near Madrid	W-Mo in skarn; W-Sn mineralisations	
45	W Spain	W mineralisation	
46	S central Spain (Cordoba)	W mineralisation (with associated As, Ag, tourmaline)	
47	NW Spain (Galicia)	W-Fe-Sn mineralisation	
48	NW Spain (Galicia)	Au and W mineralisations in granite-greisen-quartz veins	
49	N Portugal	W mineralisation in pegmatites (scheelite, wolframite); W-Sn mineralisation with associated Au (Ag)	
50	N Portugal	W-Sn-Cu-Zn mineralisation in granite and greisen	

650

651   3.3.2. Tungsten in soil as a mineral potential indicator

652

653   Tungsten anomalies in European Ap soil are most pronounced in regions with granitic

654 bedrock and associated with various types of mineralisation, especially Au (and Ag) and base

655 metals hosted by granitic rocks (Figs. 5a and b). This is typical geological environment where

656 various W ore deposits can be found, e.g., granitic intrusions in northern Portugal, Massif

657 Central in France, Bohemian Massif in Czech Republic, the Vosges Mountains in eastern

658 France and the Alpine region (mainly in Switzerland and western Austria). Scheelite and

659　wolframite (often accompanied by cassiterite and fluorspar) are the economic sources of W,

660　and they are mainly found in quartz-rich veins, pegmatites and skarn deposits. Most W deposits

661　are of metasomatic or hydrothermal origin. Tungsten is used as a pathfinder for gold deposits.

662　High W concentrations occur in Ap soil that overlies igneous and metamorphic rocks of the

663　Fennoscandian Shield, mainly of Palaeoproterozoic age. In Scandinavia, the largest W

664　anomalies occur in the Skellefte ore district, Bergslagen and sporadically along the coast of the

665　Gulf of Bothnia. These anomalies reflect known W mineralisation occurring in granite, gneiss

666　and quartz veins (together with U, Au, Ag and Li). In Lapland, anomalies occur within the so

667　called Gold Line and they follow Sn, Mo, Cu, Fe, U and precious metal ore deposits with Au

668　and Ag. The Bergslagen mining district comprises the most important W (scheelite) ore deposits

669　in Sweden, which are located mainly in skarn-limestone, commonly in contact with

670　Svecokarelian granitic rocks (Andersson et al., 2014).

671　　　　By comparison with the ProMine mineral deposit map (Table 4; Figs. 5a and b), it can

672　be observed that several strong anomalies are not reflected on the mineral deposits map, e.g.,

673　anomalies in NW Germany/Eastern Netherlands, SW Slovakia, central Italy, southern and

674　central Germany, northern Sweden and central Finland. For example, an unexpectedly

675　extensive W anomaly in central Italy (No. 31, Fig. 5b) might be related to the young volcanism.

676　Other anomalies, such as No. 18 in the Thuringian Forest indicates that mining and exploration

677　activities in this polymetallic province did not focus on W, which shows elevated soil

678　concentrations. All these observations indicate that there is a high potential for discovering new

679　W resources.

680

681　*Table 5. Explanation of Li anomalies in Europe: comparison with ProMine Mineral Database*

682　*(PMD; Cassard et al., 2012, 2015). For anomaly numbers see Fig. 6.*

No.	Country	Explanation (PMD)	Other explanation
1	E Sweden		Occurrences of LCT (Lithium-Cesium-

No.	Country	Explanation (PMD)	Other explanation
			Tantalum) pegmatites of the Varuträsk type
2	Central Sweden		Li (Sn, Ta) mineralisation (FODD database); Sn, Li, Nb, Be, Ta occurrences (SGU database)
3	Central Sweden (Bergslagen)	Li in pegmatites (spodumene, beryl, cassiterite); Li-Fe in magnetite skarn; REE and pegmatite occurrences	Lithium seems to be enriched in some Fe deposits
4	Norway (Oslo Rift)		Mineralisation in pegmatites; Mo mineralisation
5	S Finland	Ta, Be, Li, Sn in pegmatites	Rapakivi granites; Li mineralisation
6	S Finland		Rapakivi granite
7	SE Poland	unexplained	
8	SW Ukraine (Carpathians)	unexplained	
9	E Ukraine (Donetsk region)	Li mineralisation	Phosphate-Be-REE-Ta-Nb deposits; Li deposits in eastern Ukraine (petalite and spodumene in pegmatites)
10	United Kingdom (Wales)		Li-bearing secondary manganese minerals in hydrothermal ore deposits and sedimentary Mn deposits
11	United Kingdom (Cornwall)	Li and Cs in pegmatites and aplites (Li, Ta, Nb, Be)	Cornubian batholith (lithium-mica-albite-topaz granites)
12	SE Ireland (Wexford)	Li mineralisation in pegmatites; LCT pegmatites (Lithium-Cesium-Tantalum)	
13	W Germany (Northern Hesse, Sauerland, SE Dortmund)	Unexplained; coal?	Slate mining (roof slate); fluorspar and baryte mining; hard coal power plant in the region; industrial region with different types of industry (metalworking) and steel production
14	W Germany (Rhenish Slate Mts., SE Bonn)	Kaolin occurrences; phosphorites	
15	SW Germany (Saarland)	Oolitic Fe-ores; Cu-Pb-Zn mineralisation	Hard coal deposits, former hard coal power

No.	Country	Explanation (PMD)	Other explanation
			plants and iron and steel works
16	SW Germany (Central Black Forest)	Au-Ge-Ag, galena, fluorspar occurrences	Pb-Cu-Fe and Fe mineralisation, Triberger biotite granite
17	SE Germany/W Czech Republic (West Erzgebirge, Western Ore Mts.)	Numerous Li occurrences in LCT pegmatites	Li in Sn mineralisation (cassiterite-quartz association) and in Li-bearing micas in granites
18	S Czech Republic	unexplained	
19	S Austria	Li mineralisation in LCT pegmatites	
20	W Austria (Insbruck)/N Italy	Li mineralisation in LCT pegmatites	
21	E Slovenia	unexplained	
22	SE Croatia/S Bosnia & Herzegovina/Montenegro	Fe deposits (oolitic iron deposits); bauxite deposits in karst and laterite; inactive Al plant	Karst/bauxite weathering
23	W Bulgaria	Granite-controlled Au-Cu deposits with quartz veins; supergene clay deposits	
24	NW Hellas (Epirus)	Laterite related polymetallic deposits (Ni, As, Au, Co, Cr, Fe, Mg, Mn, Pd, Pt); Ophiolite related VMS deposits (Cu, Zn, Co)	Karst/bauxite weathering; correlation to mafic and ultramafic rocks (ophiolite) and Fe-Ni deposits; phosphorites; evaporites (by the coast)
25	C Hellas (Sterea Elladha)	Bauxite and Al-rich rocks deposits (in karst and laterite); mine waste dump with 'red muds' from bauxite refining	Karst/bauxite weathering? Possible correlation to mafic and ultramafic rocks and Fe-Ni deposits
26	SE Switzerland	Ta-U mineralisation in felsic alkaline rocks	Mineralisations in quartz veins, pegmatites
27	NW Italy (Genoa, Portofino)	Volcano-sedimentary Mn mineralisation with jasper and chert; Cr mineralisation in mafic-ultramafic rocks (Cu-Zn, Co VMS deposit)	
28	Central Italy (Ravenna)		Valli di Comacchio: brackish lagoons with brines which might be enriched in lithium
29	Central Italy (including island of Elba)	Li – Cs - REE mineralisation in pegmatites; Sb (+Hg) mineralisation	Related to the igneous rocks from Roman Alkaline Province
30	Italy	unexplained	

No.	Country	Explanation (PMD)	Other explanation
31	Italy (Gargano Peninsula)	Bauxite deposits and Al-rich rocks in karst/laterite	Possibly related to the plutonic and volcanic alkaline rocks (gabbro and syenite, anorogenic lamprophyres
32	Italy (Southern Apennines)	unexplained	
33	N Corsica (France)	Granitic-pegmatitic veins and greisens (W-Mo, Ag)	
34	S Belgium (Dinant, Ardennes)	Vein deposits with fluorspar, baryte, sphalerite, galena, etc; historical mining	Kaolinised regoliths
35	NW France (Hercynian Armorican Massif)	Peraluminous leucogranites, pegmatites and peri-granitic veins (associated with U, Sn, W, REE, Zr and beryl)	
36	NW France (Poitu)	Associated with W-baryte-kyanite deposits, carbonate-hosted veins with Ba and F deposits (MVT)	
37	S Central France (Massif Central)	Li mineralisation in pegmatites associated with beryl, cassiterite, Ta-Nb, Y and REE; numerous occurrences with Sn, W, Au, Ag	
38	S Central France (Massif Central)	Numerous occurrences (+Sn, As, Fe, W, Ag, Au) in granitic and peri-granitic veins and in greisens	
39	SE France (Grenoble)	Cu-Sn-Ag-Mo-Bi and baryte-fluorspar granite-controlled mineralisation; In-Zn, fluorspar mineralisation, fault-related; granitic and peri-granitic veins; historical mining	
40	S France/N Spain (Pyrenees)	W-Mo skarn mineralisation, associated with baryte; Ag, Zn and Pb; Zn-Ag, Co-Sn Pb (+Ga, Ge) mineralisation; historical mining	
41	N Spain (Zaragoza)	Clays and evaporitic salts deposits	This anomaly in south Pyrenean Zone correlates well with Li anomaly (partial extraction) in sediments in Geochemical Atlas of

No.	Country	Explanation (PMD)	Other explanation
			Spain (Locutura et al., 2012).
42	Central Spain (Madrid)	Sn, W, Ag mineralisation related to granite, pegmatite, greisen and quartz- and mica-rich (muscovite) veins; W-Mo skarn mineralisation	
43	S Central Spain	W, Sn, quartz, tourmaline; As, Fe, Ag, Au, Pb mineralisation in granite-pegmatite rocks	Related to Iberian Massif (Central Iberian Zone); the Almadén mercury mining district
44	NW Spain (Galicia)	Associated Au-As mineralisation in quartz-rich veins; Fe-Sn-W-Cu in granites and pegmatites	Hercynian granite; Li-rich mineral occurrences associated with aplite-pegmatite dykes and sills intruded in granitic and metasedimentary rocks of Galicia – Trás-os-Montes geotectonic zones
45	NW Spain (Galicia)	Associated with Au-Ag in quartz-rich veins; Sn-Ta-Nb, quartz, kaolin and REE mineralisation	Hercynian granite
46	N Portugal (Braga)	Lepidolite, spodumene, petalite mineralisation in pegmatite, associated with W-Sn-Au-Ta vein mineralization zone	Galicia - Trás-os-Montes Zone; aplite-pegmatite veins in a late Hercynian granite, rich in spodumene, embedded in Silurian metasediments
47	Central Portugal (Castelo Branco)	Li mineralisation in aplites and pegmatites, associated with W-Sn-Au, Ta-Nb, ilmenite, beryl mineralisation	The Central-Iberian Zone; aplite-pegmatite veins in a late Hercynian granite

683

684   3.3.3. Lithium in soil as a mineral potential indicator

685   Lithium in agricultural soil (Table 5, Figs. 6a and b) shows its high concentrations

686   predominantly in regions with granitic parent materials. A comparison between Li-bearing ore

687   deposits in Europe and the Ap soil geochemical map for Li reveals that many anomalies are

688   associated with Li-bearing mineralisation, especially with occurrences of LCT (Lithium-

689   Cesium-Tantalum) pegmatites, for example, in the Galicia-Trás-os-Montes zone (anomalies

690   No. 46 and 47 and in western Alps (anomaly No. 39). In NW Spain and northern Portugal, Li

691   anomalies are closely associated not only with known Li mineralisation but also with Sn, W,

692   Nb and Ta occurrences. These Li deposits in the Central Iberian Zone have been mined

693   intensively in recent years and Portugal became the world's sixth largest Li producer (Roda-

694   Robles et al., 2016). In northern Europe, high Li concentrations in Ap soil occur in regions with

695   granitic parent materials (e.g., southern Finland), but also in till overburden enriched in

696   postglacial and marine clay, for example, in central Sweden (see also Fig. 8). In southern

697   Lapland, anomalies coincide with Au, W, Mo and scheelite mineralisation of the 'Gold Line'

698   ore province. Recently, the Bergby deposit was discovered in central Sweden, which lies 25 km

699   north of the town of Gävle with Li_2O averaging 1.71% and ranging from 0.01% to 4.65%

700   (http://leadingedgematerials.com/leading-edge-materials-discovers-lithium-mineralization-in-

701   outcrop-at-bergby-project-sweden/).

702   There is a clear correlation of Li with mica- and clay-rich soil (as reflected by Ga, Al,

703   Cs, Rb) but also with some Fe-rich phases, which can be a result of both weathering and

704   presence of more mafic parent materials (correlation together with Fe, Cr, Co, Sc). High

705   correlation with chalcophile elements such as Zn, In, Tl, Cu makes geochemical behaviour of

706   Li in soil more complicated and requires careful interpretation at the regional to local scale.

707   Lithium anomalies are more difficult to follow in the ProMine Mineral Database (Cassard et

708   al., 2012, 2015). There are several relatively extensive anomalies, which do not have a direct

709   explanation with respect to the ProMine Mineral Database, e.g., Li anomaly in Wales (No. 10,

710   Fig. 6) in the United Kingdom, Li anomalies in western Germany (Nos. 13 and 14), in W Hellas

711   (Nos. 24 and 25) and in NE Spain (No. 41). Locally, high Li concentrations in Ap soil occur at

712   Lisbon city limits in the delta of the Tajo river, and in the vicinity of the brackish lagoons with

713   brines near Ravenna in Italy, and they may have secondary and even anthropogenic origin.

714 These enhanced secondary Li concentrations can be misleading when looking for economic Li

715 occurrences.

716

717 3.3.4. Combined Sb, W and Li anomalies in soil as mineral potential indicators

718

719 Table 6 summarises the co-existing anomalies for Sb, W and Li. The most

720 straightforward observation is that in several regions (Cornwall, Massif Central, Erzgebirge,

721 and the Alps) all three commodities can be found close to one another and, thus, polymetallic

722 ore provinces can be defined, even if the host rock is not of the same lithology and the ore-

723 forming processes also differ.

724

725 *Table 6. Summary of co-existing Sb, W and Li anomalies.*

Region	Sb	W	Li
Cornwall (United Kingdom)	12	13	11
Massif Central (France)	44-46	39	37-38
W Pyrennes (N Spain/S France)	48	42	40
Erzgebirge (E Germany/N Czech Republic	19	17	17
W Salzburg/Tyrol (Austria)	27	26	20
Brittany (NW France)		35	35
Central Portugal		50	47
Southern Czech Republic		18	22
SE France	47		39
NE Spain	49		41
E Ukraine	9		9
W France	43	36	
E France	40	38	

726

727

4. Conclusions

The demand for 'high-tech' element resources stimulated efforts to find new deposits and even possibilities to extract them from active and historical mines throughout the world. The GEMAS data set offers European scale results for several so-called high-tech elements, and almost all listed on the Critical Raw Materials list by the European Commission (2017). Here, three of the high-tech elements, Sb, W and Li were used as test elements. The geochemical distribution of Sb, W and Li in agricultural soil of Europe appears to be a useful starting tool for identifying areas for discovering new sources of high-tech elements. Most of the patterns observed on the geochemical maps of Sb, W and Li can be directly interpreted in terms of known ore deposits and mineralised occurrences and most of the anomalies reflect natural sources of these elements. Additionally, their spatial distribution seems to be modified by weathering type and intensity, Quaternary history and climate, like, for example, the clear difference in element concentrations between northern and southern Europe. The chemical composition of agricultural soil represents largely the primary mineralogy of the source parent material, with superimposed effects of pre- and post-depositional chemical weathering, formation of secondary products such as clays, and element mobility. For Sb, the most promising are regions with known sulphide mineralisation, while for Li and W, regions with crystalline bedrock and evolved granitic rocks should be of interest.

Natural background concentrations of Sb, W and Li in agricultural soil define areas of interest and their relationship to mineralisation, rock types and mining centres, and provide important ground for further investigations. The application of GEMAS soil data to mineral exploration is promising, especially as most of the Sb, W and Li anomalies can be explained by known and mapped mineralisation (such as the ProMine Mineral Database and national registers). In conclusion, several unexplained anomalies require more detailed geochemical

753 surveys, these could shed light on potential mineral resources that have to date remained

754 undiscovered.

755

Acknowledgments

772

References[1]

774

775 Albanese, S., Sadeghi, S., Lima, A., Cicchella, D., Dinelli, E., Valera, P., Falconi, M., Demetriades, A.,
776   De Vivo, B. and the GEMAS Project Team, 2015. GEMAS: Chromium, Ni, Co and Cu in agricultural
777   and grazing land soil of Europe. Journal of Geochemical Exploration 154, 81-93.

778 Aitchison, J., 1986. The statistical analysis of compositional data. London: Chapman & Hall, 416 pp.

779 Ali, S.H., Giurco, D., Arndt, N., Nickless, E., Brown, E., Demetriades, A., Durrheim, R, Enriquez, M.A.,
780   Kinnaird, J., Littleboy, A., Meinert, L.D., Oberhänsli, R., Salem, J., Schodde, R., Schneider, G.,
781   Vidal, O., Yakovleva, N., 2017. Mineral supply for sustainable development requires resource
782   governance. Nature 543, 367–372.

---

[1] Note: All web links checked on the 9th March 2019

783   Andersson, M., Carlsson, M., Ladenberger, A., Morris, G., Sadeghi, M., Uhlbäck, J., 2014. Geokemisk
784   atlas över Sverige (Geochemical Atlas of Sweden), Geological Survey of Sweden, 210 pp.;
785   http://doi.org/10.13140/2.1.1341.6642.

786   Bednar, A.J., Jones, W.T., Chappell, M.A., Johnson, D.R., Ringelberg, D.B., 2010. A modified acid
787   digestion procedure for extraction of tungsten from soil. Talanta 80, 1257-1263.

788   Belzile, N., Chen, Y.-W., Wang, Z., 2001. Oxidation of antimony (III) by amorphous iron and
789   manganese oxyhydroxides. Chemical Geology 174, 379-387.

790   Bertrand, G., Cassard, D., Arvanitidis, N., Stanley, G., EuroGeoSurveys Mineral Resources Expert
791   Group, 2016. Map of critical raw material deposits in Europe. Energy Procedia 97, 44-50;
792   https://doi.org//10.1016/j.egypro.2016.10.016.

793   Birke, M., Reimann, C., Rauch, U., De Vivo, B., Halamić, J., Klos, V., Gosar, M., Ladenberger, A.,
794   2014a. Distribution of Cadmium in European Agricultural and Grazing Land Soil. Chapter 5 In: C.
795   Reimann, M. Birke, A. Demetriades, P. Filzmoser, P.O'Connor (Editors), Chemistry of Europe's
796   agricultural soils – Part B: General background information and further analysis of the GEMAS data
797   set. Geologisches Jahrbuch (Reihe B103), Schweizerbarth, Hannover, 89-115.

798   Birke, M., Reimann, C., Fabian, K., 2014b. Analytical Methods Used in the GEMAS Project. Chapter
799   5 In: C. Reimann, M. Birke, A. Demetriades, P. Filzmoser, P.O'Connor (Editors), Chemistry of
800   Europe's agricultural soils – Part A: Methodology and interpretation of the GEMAS data set.
801   Geologisches Jahrbuch (Reihe B102), Schweizerbarth, Hannover, 41-46.

802   Birke, M., Rauch, U., Stummeyer, J., 2015. How robust are geochemical patterns? A comparison of low
803   and high sample density geochemical mapping in Germany. Journal of Geochemical Exploration
804   154, 105-128.

805   Birke, M., Reimann, R., Oorts, K., Rauch, U., Demetriades, A., Dinelli, E., Ladenberger, A., Halamić,
806   J. Gosar, M., Jähne-Klingberg, F., The GEMAS Project Team, 2016. Use of GEMAS data for risk
807   assessment of cadmium in European agricultural and grazing land soil under the REACH Regulation.
808   Applied Geochemistry, 74, 109-121.

809   Birke, M., Reimann, C., Rauch, U., Ladenberger, A., Demetriades, A., Jähne-Klingberg, F., Oorts, K.,
810   Gosar, M., Dinelli, E., Halamic, J., The GEMAS Project Team, 2017. GEMAS: Cadmium
811   distribution and its sources in agricultural and grazing land soil of Europe - original data versus clr-
812   transformed data. Journal of Geochemical Exploration, 173, 13-30.

813   Bölviken, B., Kullerud, G., Loucks, R.R., 1990. Geochemical and metallogenic provinces: a discussion
814   initiated by results from geochemical mapping across northern Fennoscandia. Journal of
815   Geochemical Exploration, 39, 49-90; https://doi.org/10.1016/0375-6742(90)90069-M.

816   Bowen, H.J.M., 1979. Environmental chemistry of the elements. Academic Press, London, New York,
817   333 pp.

818 Boyle, R.W., 1974. Elemental associations in mineral deposits and indicator elements of interest in

819   geochemical prospecting. Energy, Mines and Resources Canada, Geological Survey Paper 74-45, 40

820   pp.; https://doi.org/10.4095/102553.

821 Boyle, R.W., Jonasson, I.R., 1984. The geochemistry of antimony and its use as an indicator element in

822   geochemical prospecting. Journal of Geochemical Exploration 20, 223-302.

823 Bringezu, S., Potocnik, J., Schandl, H., Lu, Y., Ramaswami, A., Swillin, M., Suh, S., 2016. Multi-Scale

824   Governance of Sustainable Natural Resource Use—Challenges and Opportunities for Monitoring

825   and Institutional Development at the National and Global Level. Sustainability 2016 8, 778, 1-25.

826 Buccianti, A., Pawlowsky-Glahn, V., Mateu-Figueras, G. (Editors), 2006. Compositional data analysis

827   in the geosciences: from theory to practice. Geological Society, London, 224 pp.

828 Buchert, M., Schüler, D., Bleher, D. 2009. Critical metals for future sustainable technologies and their

829   recycling potential. DTI/1202/PA, UNEP DTIE, Sustainable Consumption and Production Branch,

830   Paris,   http://www.unep.fr/shared/publications/pdf/DTIx1202xPA-

831   Critical%20Metals%20and%20their%20Recycling%20Potential.pdf.

832 Buschmann, J., Sigg, L., 2004. Antimony(III) Binding to Humic Substances: Influence of pH and Type

833   of Humic Acid. Environmental Science & Technology 38, 4535-4541.

834 Caritat, P. de, Cooper, M., 2011a. National Geochemical Survey of Australia: Data Quality Assessment,

835   Geoscience Australia, Record 2011/21, GeoCat # 71971 vol. 1. Australian Government, Canberra,

836   pp. 1-268.

837 Caritat, P. de, Cooper, M., 2011b. National Geochemical Survey of Australia: Data Quality Assessment,

838   Geoscience Australia, Record 2011/21, GeoCat # 71971 vol. 2. Australian Government, Canberra,

839   pp. 269-478.

840 Caritat, P.de, Cooper, M., 2011c. National Geochemical Survey of Australia: The Geochemical Atlas of

841   Australia, Geoscience Australia, Record 2011/20, GeoCat # 71973 vol. 1. Australian Government,

842   Canberra, pp. 1-268.

843 Caritat, P.de, Cooper, M., 2011d. National Geochemical Survey of Australia: The Geochemical Atlas

844   of Australia, Geoscience Australia, Record 2011/20, GeoCat # 71973, vol. 2. Australian Government,

845   Canberra, pp. 269-557.

846 Cassard, D., Bertrand, G., Maldan, F., Gaàl, G., Kaija, J., Aatos, S., Angel, J.M., Arvanitidis, N., Ballas,

847   D., Billa, M., Christidis, C., Dimitrova, D., Eilu, P., Filipe, A., Gazea, E., Inverno, C., Kauniskangas,

848   E., Maki, T., Matos, J., Meliani, M., Michael, C., Mladenova, V., Navas, J., Niedbal, M., Perantonis,

849   G., Pyra, J., Santana, H., Serafimovski, T., Serrano, J.J., Strengell, J., Tasev, G., Tornos, F., Tudor,

850   G., 2012. ProMine pan-European mineral deposit database: a new dataset for assessing primary

851   mineral resources in Europe. Workshop on: Mineral Resources Potential Maps: A Tool for

852   Discovering Future Deposits. 12th–14th March 2012, Nancy, France, Proceedings, pp. 9–13.

853 Cassard, D., Bertrand, G., Billa, M., Serrano, J.J., Tourlière, B., Angel, J.M., Gaál, G., 2015. ProMine

854   mineral databases: New tools to assess primary and secondary mineral resources in Europe. Chapter

855   2 In: Weihed, P. (Editor), 3D, 4D and Predictive Modelling of Major Mineral Belts in Europe.

856   Mineral Resource Reviews. Springer International Publishing, 9-58; https://doi.org/10.1007/978-3-

857   319-17428-0_2.

858   Charlier, P., Bou Abdallah, F., Bruneau, R., Jacqueline, S., Augias, A., Bianucci R., Perciaccante A.,

859   Lippi D., Appenzeller O., Rasmussen, K.L., 2017. Did the Romans die of antimony poisoning? The

860   case of a Pompeii water pipe (79 CE), Toxicology Letters 281, 184-186.

861   Cicchella, D., Lima, A., Birke, M., Demetriades, A., Wang, X., De Vivo, B., 2013. Mapping

862   geochemical patterns at regional to continental scales using composite samples to reduce the

863   analytical costs. Journal of Geochemical Exploration 124, 79-91.

864   Cicchella, D., Albanese, S., Birke, M., De Vivo, B., De Vos, W., Dinelli, E., Lima, A., O'Connor, P.J.,

865   Salpeteur, I., Tarvainen, T., 2014. Natural Radioactive Elements U, Th and K in European

866   Agricultural and Grazing Land Soil. Chapter 8 In: C. Reimann, M. Birke, A. Demetriades, P.

867   Filzmoser, P. O'Connor (Editors), Chemistry of Europe's agricultural soils – Part B: General

868   background information and further analysis of the GEMAS data set. Geologisches Jahrbuch (Reihe

869   B103), Schweizerbarth, Hannover, 145-159.

870   Cristache, C., Comero, S., Locoro, G., Fissiaux, I., Ruiz, A.A., Tóth, G., Gawlik, B.M., 2014.

871   Comparative study on open system digestion vs. microwave-assisted digestion methods for trace

872   element analysis in agricultural soils. Joint Research Centre, Institute for Environment and

873   Sustainability,   Luxembourg,   38   pp.;

874   http://publications.jrc.ec.europa.eu/repository/bitstream/JRC90183/lb-na-26636-en-n.pdf

875   Demetriades, A., 2011. Understanding the quality of chemical data from the urban environment – Part

876   2: Measurement uncertainty in the decision-making process. Chapter 6 In: C.C. Johnson, A.

877   Demetriades, J. Locutura, R.T. Ottesen (Editors), Mapping the chemical environment of urban areas.

878   John Wiley & Sons Ltd., Chichester, U.K., 77-98. https://doi.org/10.1002/9780470670071.ch6.

879   Demetriades, A., Reimann, C., 2014. Mineral deposits of Europe. Chapter 3 In: Reimann, C., Birke,M.,

880   Demetriades, A., Filzmoser, P., O'Connor, P. (Eds.), Geologisches Jahrbuch (Reihe B 103).

881   Schweizerbarth, Hannover, 71–78.

882   Demetriades, A., Reimann, C., Filzmoser, P., 2014. Evaluation of GEMAS project quality control

883   results. Chapter 6 In: C. Reimann, M. Birke, A. Demetriades, P. Filzmoser, P. O'Connor (Editors),

884   Chemistry of Europe's agricultural soils – Part A: Methodology and interpretation of the GEMAS

885   data set Geologisches Jahrbuch (Reihe B102), Schweizerbarth, Hannover, 47-60.

886   De Vos, W., Tarvainen, T., Salminen, R., Reeder, S., De Vivo, B., Demetriades, A., Pirc, S., Batista,

887   M.J., Marsina, K., Ottesen, R.T., O'Connor, P., Bidovec, M., Lima, A., Siewers, U., Smith, B.,

888   Taylor, H., Shaw, R., Salpeteur, I., Gregorauskiene, V., Halamić, J., Slaninka, I., Lax, K., Gravesen,

889   P., Birke, M., Breward, N., Ander, E.L., Jordan, G., Duris, M., Klein, P., Locutura, J., Bel-lan, A.,

890   Pasieczna, A., Lis, J., Mazreku, A., Gilucis, A., Heitzmann, P., Klaver, G., Petersell, V., 2006.

891   Geochemical Atlas of Europe. Part 2 - Interpretation of Geochemical Maps, Additional Tables,

892 Figures, Maps, and Related Publications. Geological Survey of Finland, Espoo, 618 pp.;
893 http://weppi.gtk.fi/publ/foregsatlas/.

894 ECS, 2010. Sludge, treated biowaste and soil - Digestion for the extraction of aqua regia soluble fraction
895 of trace elements. prEN 16174, CEN/TC400 (Draft). European Committee for Standardisation,
896 Brussels, 15 pp.;
897 https://www.ecn.nl/docs/society/horizontal/BT_TF151_WI_CSS99025B_Aqua_regia_2992007.pdf
898 .

899 European Commission, 2017. Study on the review of the list of Critical Raw Materials: Criticality
900 assessments. Brussels, 13.9.2017, COM(2017) 490 final; 92 pp.; http://doi.org/10.2873/876644.

901 Fay, D., Kramers, G., Zhang, C., McGrath, D., Grennan, E. 2007. Soil Geochemical Atlas of Ireland.
902 Teagasc, Environmental Protection Agency, Wexford, 117 pp.;
903 https://www.teagasc.ie/media/website/publications/2011/Soil_Geochemical_AtlasofIreland.pdf.

904 Filzmoser, P., Reimann, C., Birke, M., 2014. Univariate Data Analysis and Mapping. Chapter 8 In: C.
905 Reimann, M. Birke, A. Demetriades, P. Filzmoser, P. O'Connor (Editors), Chemistry of Europe's
906 agricultural soils – Part A: Methodology and interpretation of the GEMAS data set. Geologisches
907 Jahrbuch (Reihe B102), Schweizerbarth, Hannover, 67-81.

908 Gál, J., Hursthouse, A., Cuthbert, S. 2007. Bioavailability of arsenic and antimony in soils from an
909 abandoned mining area, Glendinning (SW Scotland). Journal of Environmental Science and Health,
910 Part A Toxic/Hazardous Substances and Environmental Engineering 42, 1263-1274.

911 Garrett, R.G., Reimann, C., Smith, D.B., Xie, X., 2008. From geochemical prospecting to international
912 geochemical mapping: a historical overview. Geochemistry: Exploration Environment Analysis 8,
913 205-217.

914 Günther, A., Reichenbach, P., Malet, J.-P., Van Den Eeckhaut, M., Hervás, J., Dashwood, C. and
915 Guzzetti, F. 2013. Tier-based approaches for landslide susceptibility assessment in Europe
916 Landslides 10, 529-546.

917 Hockmann, K., Schulin, R., 2013. Leaching of Antimony from Contaminated Soils. In: Selim, H.M.
918 (Ed.), Competitive Sorption and Transport of Heavy Metals in Soils and Geological Media. CRC
919 Press, Boca Raton, 119-145.

920 Hu, Z., Gao, S., 2008. Upper crustal abundances of trace elements: A revision and update. Chemical
921 Geology 253, 205–221.

922 Hubbert, M.K., 1982. Techniques of Prediction as Applied to Production of Oil and Gas. In: Gass, S.I.
923 (Editor), Oil and Gas Supply. US Department of Commerce, NBS Special Publication 631, May
924 1982.

925 Johnson, C.A., Moench, H., Wersin, P., Kugler, P., Wenger, C., 2005. Solubility of Antimony and Other
926 Elements in Samples Taken from Shooting Ranges. Journal of Environmental Quality 34, 248-254.

927 Jordan, G., Petrik, A., De Vivo, B., Albanese, S., Demetriades, A., Sadeghi, M., The GEMAS Project
928 Team, 2018. GEMAS: Spatial analysis of the Ni distribution on a continental-scale using digital

929   image processing techniques on European agricultural soil data. Journal of Geochemical
930   Exploration186, 143-157.

931   Kabata-Pendias, A., Mukherjee, A.B., 2007. Trace Elements from Soil to Human. Springer Verlag,
932   Berlin, Heidelberg, 550 pp.

933   Koutsospyros, A., Braida, W., Christodoulatos, C., Dermatas, D., Strigul, N. 2006. A review of tungsten:
934   From environmental obscurity to scrutiny. Journal of Hazardous Materials 136, 1-19.

935   Ladenberger, A., Andersson, M., Reimann, C., Tarvainen, T., Filzmoser, P., Uhlbäck, J., Morris, G.,
936   Sadeghi , M. 2013. Geochemical mapping of agricultural soils and grazing land (GEMAS) in
937   Norway, Finland and Sweden – regional report. Geological Survey of Sweden, SGU-rapport
938   2012:17, 160 pp.; http://resource.sgu.se/produkter/sgurapp/s1217-rapport.pdf;
939   https://www.researchgate.net/publication/260872161_Geochemical_mapping_of_agricultural_soils
940   _and_grazing_land_GEMAS_in_Norway_Finland_and_Sweden_-_regional_report.

941   Ladenberger, A., Demetriades, A., Reimann, C., Birke, M., Sadeghi, M., Uhlback, J., Andersson, M.,
942   Jonsson, E., the GEMAS Project Team. 2015. GEMAS: Indium in agricultural and grazing land soil
943   of Europe – its source and geochemical distribution patterns. Journal of Geochemical Exploration
944   154, 61–80.

945   Ladenberger, A., Uhlbäck, J., Andersson, M., Reimann, C., Tarvainen, T., Morris, G., Sadeghi, M.,
946   Eklund, M., Filzmoser, P., 2014. Elemental Patterns in Agricultural and Grazing Land soil in
947   Norway, Finland and Sweden: What have we learned from continental-scale mapping? Chapter 14
948   In: C. Reimann, M. Birke, A. Demetriades, P. Filzmoser, P. O'Connor (Editors), Chemistry of
949   Europe's agricultural soils – Part B: General background information and further analysis of the
950   GEMAS data set. Geologisches Jahrbuch (Reihe B103), Schweizerbarth, Hannover, 235-251.

951   Lambert, I., Durrheim, R., Godoy, M., Kota, M., Leahy, P., Ludden, J., Nickless, E., Oberhaensli, R.,
952   Anjian, W., Williams, N. 2013. Resourcing Future Generations: A proposed new IUGS initiative.
953   Episodes 36, 82-86.

954   Locutura, J., Bel-lan, A., García, C.A., Martínez, S., 2012. Atlas Geoquímico de España. Instituto
955   Geológico y Minero de España, Madrid, 592 pp. (A3 size);
956   http://www.igme.es/actividadesIGME/lineas/CartoGeo/geoquimica/geoquimicaIng.htm.

957   Meinert, L.D., Robinson, G.R., Nassar, N.T., 2016. Mineral resources: reserves, peak production and
958   the future. Resources 5, 14.

959   Millot R., Vigier, N., Gaillardet, J., 2010. Behaviour of lithium and its isotopes during weathering in the
960   Mackenzie Basin, Canada. Geochimica et Cosmochimica Acta 74, 3897–3912.

961   Négrel, Ph., Sadeghi, M., Ladenberger, A., Reimann, C., Birke, M., the GEMAS Project Team. 2015.
962   Geochemical fingerprinting and sources discrimination in soils and sediments at continental scale.
963   Chemical Geology 396, 1-15.

964 Négrel, Ph., Ladenberger, A., Reimann, C., Birke, M., Sadeghi, M., the GEMAS Project Team. 2016.
965   GEMAS: source, distribution patterns and geochemical behavior of Ge in agricultural and grazing
966   land soils at European continental scale. Applied Geochemistry 72, 113-124.

967 Négrel, Ph., De Vivo, B., Reimann, C., Ladenberger, A., Cicchella, D., Albanese, S., Birke, M., De Vos,
968   W., Dinelli, E., Lima, A., O'Connor, P.J., Salpeteur, I., Tarvainen, T., the GEMAS Project Team,
969   2018a. U-Th signatures of agricultural soil at the European continental scale (GEMAS): Distribution,
970   weathering patterns and processes controlling their concentrations. Science of the Total Environment
971   622-623, 1277-1293.

972 Négrel, Ph., Ladenberger, A., Reimann, C., Birke, M., Sadeghi, M., the GEMAS Project Team., 2018b.
973   Distribution of Rb, Ga and Cs in agricultural land soils at European continental scale (GEMAS):
974   Implications for weathering conditions and provenance. Chemical Geology 479, 188-203.

975 Nickless, E., Ali, S., Arndt, N., Brown, G., Demetriades, A., Durrheim, R., Enriquez M.A., Giurco, D.,
976   Kinnaird, J., Littleboy, A., Masotti, F., Meinert, L., Nyanganyura, D., Oberhänsli, R., Salem, J.,
977   Schneider, G., Yakovleva., N., 2015. Resourcing Future Generations: A Global Effort to Meet The
978   World's Future Needs Head-on. International Union of Geological Sciences, 76 pp.;
979   http://iugs.org/uploads/RFG%20Report-sm.pdf.

980 Ottesen, R.T., Birke, M., Finne, T.E., Gosar, M., Locutura, J., Reimann, C., Tarvainen, T., the GEMAS
981   Project team. 2013. Mercury in European agricultural and grazing land soils. Applied Geochemistry
982   33, 1-12.

983 Pawlowsky-Glahn, V., Buccianti, A., 2011. Compositional data analysis: theory and applications.
984   Wiley, Chichester, 378 pp.

985 Plant, J.A., Breward, N., Forrest, M.D., Smith, R T., 1989. The gold pathfinder elements As, Sb and Bi:
986   their distribution and significance in the south-west Highlands of Scotland. Transactions of the
987   Institution of Mining & Metallurgy (Section B: Applied earth science) 98, B91-B101.

988 Poňavič, M., Scheib, A., 2014. Distribution of Selenium in European Agricultural and Grazing Land
989   Soil. Chapter 7 In: C. Reimann, M. Birke, A. Demetriades, P. Filzmoser, P. O'Connor (Editors),
990   Chemistry of Europe's agricultural soils – Part B: General background information and further
991   analysis of the GEMAS data set. Geologisches Jahrbuch (Reihe B103), Schweizerbarth, Hannover,
992   131-144.

993 Rawlins, B.G., McGrath, S.P., Scheib, A.J., Breward, N., Cave, M., Lister, T.R., Ingham, M., Gowing,
994   C., Carter, S., 2012. The advanced soil geochemical atlas of England and Wales. British Geological
995   Survey, Nottingham, UK, 227 pp.

996 Reimann, C., Siewers, U., Tarvainen, T., Bityukova, L., Eriksson, J., Giucis, A., Gregorauskienė, V.,
997   Lukashev, V.K., Matinian, N.N., Pasieczna, A., 2003. Agricultural Soils in Northern Europe - A
998   Geochemical Atlas (Baltic Soil Survey), Geologisches Jahrbuch Sonderhefte Reihe D, Heft 5.
999   Schweizerbart Science Publishers, Stuttgart, 279 pp.

1000   Reimann, C., Arnoldussen, A., Englmaier, P., Filzmoser, P., Finne, T.E., Garrett, R.G., Koller, F.,
1001   Nordgulen, Ø., 2007a. Element concentrations and variations along a 120 km long transect in south
1002   Norway – anthropogenic *vs.* geogenic *vs.* biogenic element sources and cycles. Applied
1003   Geochemistry 22, 851–871.

1004   Reimann, C., Melezhik, V., Niskavaara, H., 2007b. Low-density regional geochemical mapping of gold
1005   and palladium highlighting the exploration potential of northernmost Europe. Economic Geology,
1006   102, 327-334.

1007   Reimann, C., Demetriades, A., Eggen, O.A., Filzmoser, P., The EuroGeoSurveys Geochemistry Expert
1008   Group, 2009. The EuroGeoSurveys geochemical mapping of agricultural and grazing land soils
1009   project (GEMAS) – Evaluation of quality control results of aqua regia extraction analysis. Geological
1010   Survey   of   Norway,   Trondheim,   NGU   report   2009.049,   94   pp.
1011   http://www.ngu.no/upload/Publikasjoner/Rapporter/2009/2009_049.pdf.

1012   Reimann, C., Matschullat, J., Birke, M., Salminen, R. 2010. Antimony in the environment: Lessons from
1013   geochemical mapping. Applied Geochemistry 25, 175–198.

1014   Reimann, C., Demetriades, A., Eggen, O.A., Filzmoser, P., EuroGeoSurveys Geochemistry Working
1015   Group, 2011. The EuroGeoSurveys geochemical mapping of agricultural and grazing land soils
1016   project (GEMAS) – Evaluation of quality control results of total C and S, total organic carbon (TOC),
1017   cation exchange capacity (CEC), XRF, pH, and particle size distribution (PSD) analysis. NGU
1018   Report   2011.043.   Geological   Survey   of   Norway,   Trondheim,   92   pp.;
1019   http://www.ngu.no/upload/Publikasjoner/Rapporter/2011/2011_043.pdf.

1020   Reimann, C., Caritat, P. de, GEMAS Project Team, NGSA Project Team, 2012a. New soil composition
1021   data for Europe and Australia: Demonstrating comparability, identifying continental-scale processes
1022   and learning lessons for global geochemical mapping. The Science of the Total Environment 416,
1023   239-252.

1024   Reimann, C., Flem, B., Fabian, K., Birke, M., Ladenberger, A., Négrel, Ph., Demetriades, A.,
1025   Hoogewerff, J., the GEMAS Project Team, 2012b. Lead and lead isotopes in agricultural soils of
1026   Europe - the continental perspective. Applied Geochemistry 27, 532–542.

1027   Reimann, C., Demetriades, A., Birke, M., Eggen, O. A., Filzmoser, P., Kriete, C., EuroGeoSurveys
1028   Geochemistry Expert Group, 2012c. The EuroGeoSurveys Geochemical Mapping of Agricultural
1029   and grazing land Soils project (GEMAS) – Evaluation of quality control results of particle size
1030   estimation by MIR prediction, Pb-isotope and MMI® extraction analyses and results of the GEMAS
1031   ring test for the standards Ap and Gr. Geological Survey of Norway, Trondheim, NGU report
1032   2012.051, 136 pp. http://www.ngu.no/upload/Publikasjoner/Rapporter/2012/2012_051.pdf.

1033   Reimann,C., Filzmoser, P., Fabian, K., Hron, K., Birke, M., Demetriades, A., Dinelli, E., Ladenberger,
1034   A., the GEMAS Project Team, 2012d. The concept of compositional data analysis in practice - Total
1035   major element concentrations in agricultural and grazing land soils of Europe. Science of the Total
1036   Environment, 426, 196–210.

1037   Reimann, C., Birke, M., Demetriades, A., Filzmoser, P., O'Connor, P. (Editors), 2014a. Chemistry of
1038   Europe's agricultural soils – Part A: Methodology and interpretation of the GEMAS dataset.
1039   Geologisches Jahrbuch (Reihe B), Schweizerbarth, Stuttgart, 528 pp.

1040   Reimann, C., Birke, M., Demetriades, A., Filzmoser, P., O'Connor, P. (Editors), 2014b. Chemistry of
1041   Europe's agricultural soils – Part B: General background information and further analysis of the
1042   GEMAS dataset. Geologisches Jahrbuch (Reihe B), Schweizerbarth, Stuttgart, 352 pp.

1043   Reimann, C., Ladenberger, A., Birke, M., Caritat, P. de, 2016. Low density geochemical mapping and
1044   mineral exploration: application of the mineral system concept. Geochemistry: Exploration
1045   Environment Analysis 16, 48-61

1046   Roda-Robles, E., Pesquera, A. Gil-Crespo, P.P., Vieira, R., Lima A., Garate-Olave, I., Martins, T.,
1047   Torres-Ruiz, J., 2016. Geology and mineralogy of Li mineralization in the Central Iberian Zone
1048   (Spain and Portugal). Mineralogical Magazine 80, 103–126.

1049   Sadeghi, M., Petrosino, P., Ladenberger, A., Albanese, S., Andersson, M., Morris, G., Lima, A.M., De
1050   Vivo, B., the GEMAS Project Team, 2013. Ce, La and Y concentrations in agricultural and grazing-
1051   land soils of Europe. Journal of Geochemical Exploration 133, 202-213.

1052   Salminen, R., Tarvainen, T., Demetriades, A., Duris, M., Fordyce, F.M., Gregorauskiene, V., Kahelin,
1053   H., Kivisilla, J., Klaver, G., Klein, P., Larson, J.O., Lis, J., Locutura, J., Marsina, K., Mjartanova, H.,
1054   Mouvet, C., O'Connor, P., Odor, L., Ottonello, G., Paukola, T., Plant, J.A., Reimann, C., Schermann,
1055   O., Siewers, U., Steenfelt, A., Van Der Sluys, J., Williams, L., 1998. FOREGS Geochemical
1056   Mapping Field Manual. Geological Survey of Finland, Espoo, Guide 47, 36 pp.;
1057   http://tupa.gtk.fi/julkaisu/opas/op_047.pdf.

1058   Salminen, R., Batista, M.J., Bidovec, M., Demetriades, A., De Vivo, B., De Vos, W., Ďuriš, M., Gilucis,
1059   A., Gregorauskienė, V., Halamić, J., Heitzmann, P., Lima, A., Jordan, G., Klaver, G., Klein, P., Lis,
1060   J.z., Locutura, J., Marsina, K., Mazreku, A., O'Connor, P., Olsson, S.Å., Ottesen, R.T., Petersell, V.,
1061   Plant, J.A., Reeder, S., Salpeteur, I., Sandström, H., Siewers, U., Steenfelt, A., Tarvainen, T., 2005.
1062   Geochemical atlas of Europe. Part 1 – Background information, methodology and maps. Geological
1063   Survey of Finland, Espoo, 525 pp.; http://weppi.gtk.fi/publ/foregsatlas/.

1064   Scheib, A.J, Flight, D.M.A., Birke, M., Tarvainen, T., Locutura, J., GEMAS Project Team, 2012. The
1065   geochemistry of niobium and its distribution and relative mobility in agricultural soils of Europe.
1066   Geochemistry: Exploration Environment Analysis 12, 293-302.

1067   Smith, D.B., Reimann, C. 2008. Low-density geochemical mapping and the robustness of geochemical
1068   patterns. Geochemistry: Exploration Environment Analysis 8, 219–227.

1069   Smith, D.B., Cannon, W.F., Woodruff, L.G., Solano, F., Kilburn, J.E., Fey, D.L., 2013. Geochemical
1070   and Mineralogical Data for Soils of the Conterminous United States, Data Series 801. U.S.
1071   Geological Survey, Reston, 19 pp.

1072   Smith, D.B., Cannon, W.F., Woodruff, L.G., Solano, F., Ellefsen, K.J., 2014. Geochemical and
1073   Mineralogical Maps for Soils of the Conterminous United States, Open-File Report 2014–1082. U.S.
1074   Geological Survey, Denver, 386 pp.

1075   Takahashi, T., Shozugawa, K., Matsuo, M., 2010. Contribution of Amorphous Iron Compounds to
1076   Adsorptions of Pentavalent Antimony by Soils. Water, Air, and Soil Pollution 208, 165-172.

1077   Tarvainen, T., Albanese, S., Birke, M., Ponavic, M. Reimann, C., the GEMAS Project Team, 2013.
1078   Arsenic in agricultural and grazing land soils of Europe. Applied Geochemistry 28, 2-10.

1079   Tardy, Y., Krempp, G., Trauth, N., 1972. Le lithium dans les minéraux argileux des sédiments et des
1080   sols. Geochimica et Cosmochimica Acta 36, 397-412.

1081   Teske, S. (Editor), 2019. Achieving the Paris Climate Agreement Goals: Global and Regional 100%
1082   Renewable Energy Scenarios with Non-energy GHG Pathways for +1.5°c and +2°C. Springer Open,
1083   491 pp.; https://doi.org/10.1007/978-3-030-05843-2.

1084   Tóth, G., Hermann, T., Szatmári, G., Pásztor, L., 2016. Maps of heavy metals in the soils of the European
1085   Union and proposed priority areas for detailed assessment. Science of The Total Environment 565,
1086   1054-1062.

1087   UNEP, 2009. Critical metals for future sustainable technologies and their recycling potential. UNEP,
1088   DTI/1202/PA, Paris, 81 pp.; http://www.unep.fr/shared/publications/pdf/DTIx1202xPA-
1089   Critical%20Metals%20and%20their%20Recycling%20Potential.pdf.

1090   Wedepohl, K.H., (Exec. Ed.), 1978. Handbook of Geochemistry. Volume II/5. Springer-Verlag, Berlin,
1091   Heidelberg, New York, 4400+ pp.

1092   Xie, X., Ren, T., Sun, H., 2012. Geochemical Atlas of China. Institute of Geophysical and Geochemical
1093   Exploration, Langfang, China, 135 pp.

1094   Zeeberg, J.J., 1998. The European sand belt in Eastern Europe – and comparison of Late Glacial dune
1095   orientation with GCM simulation results. Boreas 27, 127–139.

1096